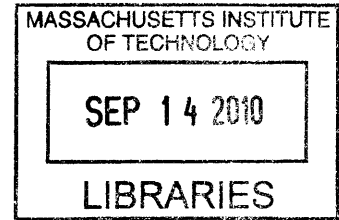


A Bicycle Electric Assist Unit  
*by Arthur Petron*

B.Sc. Massachusetts Institute of Technology 2008



**ARCHIVES**

Submitted to the Program in Media Arts and Sciences,  
School of Architecture and Planning,  
in partial fulfillment of the requirements for the degree of  
Master of Science  
at the MASSACHUSETTS INSTITUTE OF TECHNOLOGY  
September 2010  
©Massachusetts Institute of Technology 2010. All rights reserved.

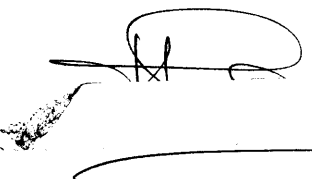
*Author:* \_\_\_\_\_ 

\_\_\_\_\_ 

Program in Media Arts and Sciences September 2010

*Certified by:* \_\_\_\_\_ 

Professor Mitchel Resnick on behalf of Professor William J. Mitchell  
Professor of Media Arts and Sciences  
Program in Media Arts and Sciences  
Thesis supervisor

*Accepted by:* \_\_\_\_\_ 

Professor Patricia Maes  
Professor of Media Arts and Sciences  
Program in Media Arts and Sciences

A Bicycle Electric Assist Unit  
*by Arthur Petron*

B.Sc. Massachusetts Institute of Technology 2008

Submitted to the Program in Media Arts and Sciences,

School of Architecture and Planning,  
in partial fulfilment of the requirements for the degree of  
Master of Science  
at the MASSACHUSETTS INSTITUTE OF TECHNOLOGY  
September 2010  
©Massachusetts Institute of Technology 2010. All rights reserved.

---

ABSTRACT

The BEAU is an electric-assist bicycle system that is completely self-contained within the rear wheel. The purpose of approaching a electric-assist bicycle in this manner is two-fold: simplifying the device and opening the method of implementation to more creative uses. The project requires a large amount of knowledge from many fields. Based on the limits of research, the project will show the aspects of the BEAU's design and how they meet the overall design goals of the project.

The BEAU is made up of several parts, none of which include a bicycle. The design of the BEAU takes the bicycle and rider into account only for aesthetic and control reasons. Inside the BEAU reside a custom motor, closed loop controller with power electronic drive elements for the motor, battery pack with custom battery management circuitry, and torque and rotary position encoders.

The simplification of both the device required to electrify a bicycle and the user input required to control such a device is intended to make the BEAU a very attractive electric bicycle conversion alternative that can be used not only for consumer uses, but also in situations of mass utilization, such as a bike sharing program.

This research was completed entirely within the Smart Cities group by the author. The original concept of the BEAU was arrived at during a meeting with the late William J. Mitchell as the "GreenWheel" and the project was begun as a team effort with Michael T. Lin, also of Smart Cities. The BEAU manifestation is entirely of the authors design with the purpose of investigating some of the more theoretical aspects of the GreenWheel concept.

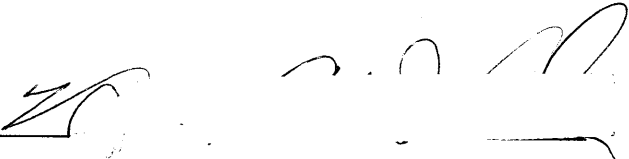
Thesis supervisor:  
Professor William J. Mitchell  
*Professor of Media Arts and Sciences*  
Program in Media Arts and Sciences

A Bicycle Electric Assist Unit

by Arthur Petron

Thesis reader:

---

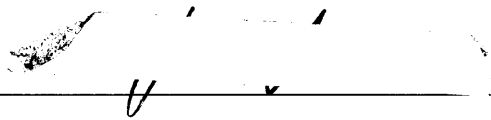


Dr. David Wallace  
*Professor of Mechanical Engineering*  
MIT Department of Mechanical Engineering

A Bicycle Electric Assist Unit

by *Arthur Petron*

Thesis reader:

A handwritten signature in black ink, appearing to read "H. Herr", is written over a horizontal line.

Professor Hugh M. Herr  
*Associate Professor of Media Arts and Sciences*  
Program in Media Arts and Sciences



---

## ACKNOWLEDGEMENTS

**William J Mitchell** The guidance of Professor Mitchell over the past two and a half years have been an invaluable experience that has taught me much about the world in which we live. I am honored to have had the chance have known Bill.

**Hugh Herr and David Wallace** My readers were very helpful throughout my term in working with the BEAU. Their advice and guidance is much appreciated.

**David Parks** Professor Parks was kind enough to review some of the more intricate methodologies of beam theory, allowing the flexure analysis to remain as closed form as possible.

**Martin Culpepper** Professor Culpepper was kind enough to steer me in the correct direction at the beginning of the flexure design process.

**Alex Slocum and Julio Guerrero** Professor Slocum and Dr. Guerrero were helpful during the beta prototype design phase in helping to keep designs manufacturable inexpensively and easily.

**Tim Robertson and Irene Zhou** My UROPs have been a wonderful help right when I needed it. They both have worked diligently this past term and summer.

**Grant Elliott** Thanks for attempting to keep me from digressing too far from the topic at hand when I come to you about something only slightly tangentially related to my thesis work asking questions.

**Sam Duffley, Chris Pentacoff, Emily Obert, Andy Marecki, Kashika Sharma, Josh Siegel, Steve Sprague at Proto Laminations, Tom Lutz, John DiFrancesco, Becky Kusko, Caroline Figgatt, Nadya Peek**

Thanks!



---

## CONTENTS

<b>1</b>	<b>Introduction</b>	<b>7</b>
1.1	Meet the BEAU . . . . .	7
1.1.1	How the BEAU works . . . . .	8
1.1.2	Inside the BEAU . . . . .	9
1.2	The BEAU and electric bikes . . . . .	10
1.2.1	Control Methods and Physical Size . . . . .	10
1.2.2	Motor Output Power . . . . .	11
1.3	Goals of the BEAU . . . . .	12
<b>2</b>	<b>The Design of the BEAU</b>	<b>15</b>
2.1	Encoder Placement . . . . .	16
2.1.1	The Magnetic Encoder . . . . .	17
2.1.2	The Optical Encoder . . . . .	17
2.2	Casing Torque and Force Analysis . . . . .	18
2.3	Internal Assembly . . . . .	18
2.4	Aesthetics . . . . .	20
<b>3</b>	<b>The Motor</b>	<b>23</b>
3.1	Motor Design Basics . . . . .	23
3.1.1	Air Gap Flux Density . . . . .	23
3.1.2	Motor Torque . . . . .	25
3.2	Theory Analysis and Verification . . . . .	26
3.2.1	FEA Results - Graphs . . . . .	26
3.2.2	FEA Results - Plots . . . . .	29
<b>4</b>	<b>Control of the BEAU</b>	<b>31</b>
4.1	Control Approach . . . . .	31
4.1.1	Torque Sensor Selection . . . . .	32
4.1.2	System Dynamics . . . . .	33
4.2	Control Implementation . . . . .	34

4.2.1	The Electrical Equations . . . . .	35
4.2.2	The Dynamic Equations . . . . .	36
4.2.3	The Closed-Loop Controller . . . . .	37
4.3	Control Hardware . . . . .	38
4.3.1	Controller Inputs and Outputs . . . . .	39
4.3.2	The Control Board and Components . . . . .	42
<b>5</b>	<b>The Torque Sensor</b>	<b>47</b>
5.1	Introduction to Flexures . . . . .	47
5.1.1	Advantages of Flexures . . . . .	48
5.1.2	Disadvantages of Flexures . . . . .	48
5.2	The Radial Flexure Design and Theory . . . . .	49
5.2.1	Physical Envelope Definition . . . . .	50
5.2.2	Basic Beam Theory . . . . .	50
5.2.3	Cartesian Beam Bending Due to Rotation . . . . .	52
5.2.4	The Effects of Shear and Strain . . . . .	55
5.2.5	Fully-Stressed Beams . . . . .	57
5.3	Radial Flexure Fabrication . . . . .	58
<b>6</b>	<b>Evaluation and Conclusion</b>	<b>63</b>

---

## 1.0. AN INTRODUCTION TO THE BICYCLE ELECTRIC ASSIST UNIT

---

### 1.1. MEET THE BEAU

Today, the term electric bicycle brings a well-understood concept to mind. A bicycle with some combination of electric motor and batteries provides complete or partial motive power to the rider. Nation-wide more than 200,000 electric bikes (e-bikes) are sold each year [10]. They are rapidly gaining in popularity especially in urban areas because of rising fuel prices, limited parking spaces, and daily traffic congestion. Ranging in price from \$300 to well over \$5,000, the variety of e-bikes for consumers is quite large[22].

Despite their popularity, e-bikes remain in the technological realm akin to the first cellphones; a headset connected by a wire to a large box containing electronics and batteries. The physical design and layout of most e-bike systems necessitates the use of a particular bicycle, and those that do not require the addition of bulky battery packs on the frame or over the wheel to power the crank-shaft or wheel mounted motor. Just as moving the cell phone to a single, hand-held device transformed it from a semi-portable, briefcase sized device to a pocket item, an electric bike whose components resided only where necessary has the potential to revolutionize the market by removing the restriction of bicycle type and allowing for creative mobility architectures that otherwise would not be possible.

The bicycle electric assist unit (BEAU) developed with the Smart Cities group under professor William J. Mitchell is a fully self-contained electrically powered torque assist unit for use with bicycles. It attaches inside the rear wheel of a standard bicycle (road or mountain style) and it ridden just like a normal bicycle. The BEAU is similar to common electric bicycles and electric bicycle kits that are currently on the market in the gross end result of its interaction with the user, however the BEAU aims to solve several problems with electric bicycle (e-bike) systems that are currently on the market in order to make the e-bike a more commonly used vehicle – ideally a vehicle that becomes preferred over a gasoline powered vehicle for certain types of trips.

While fully self-contained system does imply the independence from *any* input, the BEAU does have an external charging port for quick recharge, as well as a data port for diagnostics, firmware upgrades, and behavior programming. These temporary electrical connections aside, during normal operation the BEAU requires no other modification, addition, or subtraction to its host bicycle beyond the wheel to function properly. The BEAU has no ON/OFF switch, no external battery packs, no hand-grip controls, no set-up procedures, and no calibration. Just get on and ride.



Figure 1.1: A depiction of the BEAU in its intended use scenario.

#### 1.1.1. HOW THE BEAU WORKS

The BEAU works by measuring the rider's torque input to the bicycle and providing a ratiometric assist torque from the motor. The rider and motor act in parallel to the wheel. This means that both the rider and motor have a direct coupling to the wheel, however the rider's coupling is unidirectional due to the presence of a freewheel sprocket on the BEAU hub's chain drive. A parallel drive has several benefits, but also presents certain control difficulties. One of these difficulties manifests by requiring that the motor assist torque never be higher than the torque that the rider supplies to the wheel at any given time without freewheeling the bicycle and consequently driving the bicycle with no power input from the rider. While riding under only motor power may be a desired effect in certain situations it causes a lack of control and "feel for the road" that is offered by bicycle riding. In general motoring without pedaling turns a bicycle into an electric scooter.

Although the motor torque can never be higher than the rider input torque, this still accounts for an effective doubling of the rider's input power at the road. This tight control of input versus output allows the rider to feel a direct connection with the road and bicycle – almost as if the electric assist were not present. A BEAU equipped bicycle should feel like a bicycle in low gear that goes the speed of a bicycle in high gear. The ability to ride faster, or at the same speed with less effort while maintaining the feel of an unmodified cycling experience is the goal of the BEAU.

### 1.1.2. INSIDE THE BEAU

The main components of the BEAU are as follows:

1. Motor - 800W peak, 24-slot, 32-pole, three-phase, frameless, brushless DC torque motor (BLDC motor).
2. Batteries - 39.6V nominal (40V peak) 4.6Ah battery pack – 182Wh with nominal charge.
3. Battery Management - 12 cell balancing, charging and protection circuitry.
4. Motor Control - Closed loop control of the motor from sensors to PWM drive signals.
5. Torque Sensor - Flexure-based torque sensing of the rider's input power

The motor is a custom designed actuator to provide the high torque constant required by the BEAU without the need for gearing. It resides in the outermost region inside the BEAU's casing – which incidentally is also the motor casing. The 800W peak power output is just over 1 horsepower. The motor is designed to run at 300 rpm at a torque consistent with the torque required to move a bicycle and rider through the air at that speed on level ground. The actual peak speed of the BEAU may vary depending on chain gearing and tire size.

The batteries in the BEAU are 3.3V 2.3Ah lithium-nanophosphate cells made by A123 Technologies. They offer very high cycle life and extremely high power density, allowing for high peak currents and high charge rates. A123 cells also have adequate heat tolerance and safe heat response which make them ideal for placement inside the motor casing where temperatures may reach above ambient levels.

Battery balancing, management, and control is handled by a custom printed circuit board (PCB) powered by an Atmel ATMEGA168 microprocessor and a pair of Intersil Technologies battery balancing integrated circuits. The circuit is able to report statistics such as battery health, charge level, discharge rate, etc to the BEAU's main control system. Battery management is necessary to prevent the cells in the BEAU from becoming charged unequally.

Using a torque request by the user, the motor control system consists of a custom printed circuit board driven by an Atmel ATMEGA165PA microprocessor in conjunction with an Allegro Microtechnologies A4935 automotive MOSFET driver integrated circuit. The PCB handles sensor input processing and conditioning, power switching for motor phasing, and closed loop control between the requested torque and the output torque of the motor.

In order to get an accurate torque request from the user, the BEAU implements a flexure-based torque sensor that is located between the freewheel and the motor casing. In this location the sensor is able to measure only the torque the user is putting into the bicycle by being outside of the motor to wheel force tree.



## 1.2. THE BEAU AND ELECTRIC BIKES

Current electric bicycles that are on the market can be classified into two categories: bike modifications and custom bicycles. Bike modifications usually come in the form of kits for purchase that the consumer can use to convert his or her already existing bicycle into an electric bicycle. Custom bicycles are full bikes that have built in components that cannot easily be made into a kit. The BEAU falls into the kit e-bike category. A comparison of the BEAU versus other e-bikes that are currently on the market can be seen in Table 1.1. To note are the bolded entries in the table.

Table 1.1: This table depicts the BEAU in comparison to the BionX, Schwinn, GreenLine and UltraMotor electric bicycles.

Feature	<b>BEAU</b>	BionX	Schwinn	GreenLine	UltraMotor
Battery Cycle Life	<b>2500</b>	800	2000	800	800
Range	<b>15-25 miles</b>		<b>25-30 mi</b>	20 mi	20 mi
Motor Power	<b>800W</b>	500W	180 W	250W	500W
Fits any Bike	<b>Yes</b>	No	No	No	No
Top Speed	<b>30 mph</b>	25 mph	??	15 mph	20 mph
Data Logging	<b>Yes</b>	No	No	No	No
Torque Sensing	<b>Yes</b>	No	No	No	No
Water Proof	<b>Yes</b>	No	<b>Yes</b>	<b>Yes</b>	<b>Yes</b>
Integrated Battery Protection	<b>Yes</b>	No	No	No	<b>Yes</b>
Regenerative Braking	No	No	No	No	No
Charge Time	<b>15 minutes</b>	??	30 minutes	??	3.5 Hours

### 1.2.1. CONTROL METHODS AND PHYSICAL SIZE

In terms of control, both kit and custom e-bikes rely on some sort of throttle for motor input. Some even feature a type of cruise control. The end result of all of these motor power input methods is the transition from a bicycle to a scooter. It is the goal of the BEAU to add to the bicycle riding experience in a way that makes riders feel as though they are still riding a device that behaves just like a bicycle. The reason for this goal (aside from the obvious: *form follows function*) is based on the learning curve associated with learning how to ride a new type of mobility device. An electric assist system which mimics the function of a normal bicycle will not require any new knowledge to use properly. It looks like a bike; it functions like a bike.

Figure 1.2 shows one disadvantage to current electric bicycle kits. Aside from the fact that many of them use sealed lead-acid batteries for energy storage – causing undue weight increase, these kits add many external components to the frame of the bicycle. In some cases these extra components can change the riding characteristics of the bike by adding a large mass to the bicycle or taking up





Figure 1.2: This is a good representation of the typical e-bike kit contents. In order to transform an existing bicycle into an electric bicycle, the wheel must be re-spoked with the new hub motor and the rest of the components must be mounted and wired to the frame of the bike.

space that was needed for another function.

In the case of non-kit e-bikes, the frame of the bicycle is usually modified in order to contain the batteries and electronics required for electric assist. While this does solve the frame infringement issue of the kits, the need for a custom designed bicycle is often more costly. Non-kit e-bikes are aesthetically functionally superior to kit types, but they still suffer from the same control scheme used in almost all electric bikes.

The closest bicycle that is comparable to the BEAU in functionality is the Giant Twist Freedom DX (pictured in Figure 1.3). It uses an integrated torque sensor to measure the rider's input torque in a similar way to the BEAU. In this way it acts to supplement the rider's pedal power rather than to replace it. The Giant Twist features a 18Ah, 24V battery pack consisting of 2 9Ah lithium-ion battery packs on either side of the rear wheel. The 250W drive motor is located on the front wheel. This is a good example of the state-of-the-art for an electric bicycle of this type.

### 1.2.2. MOTOR OUTPUT POWER

The amount of energy a rider must put into his or her bicycle changes with several environmental factors. The two largest factors that change the energy required to move forward at a selected speed are wind and terrain slope. On a windless day the air resistance is fairly small unless the rider is traveling at higher speeds. The difference between slope and wind speed becomes immediately apparent during hill climbing. The energy increase for a change in speed on a slope generally increases much more steeply than for simply a change in wind speed.



Figure 1.3: The Giant Twist Freedom DX Electric Bicycle. In terms of currently on the market electric bicycles, this is a good example of the state-of-the-art.

This effect can be seen quite easily in Figure 1.4. A slope of only three degrees at a speed of 5mph requires as much energy as traveling at 20mph on level ground. Most electric bike motors are between 150W and 500W, with the mode being around 200W. With the trend in e-bikes being to scooter rather than supplement pedal power, a 200W bicycle will not allow for easy ascent of slopes at a reasonable speed. The BEAU's motor is rated at a high peak power with the hopes of avoiding this. A cyclist who only uses a bicycle for pleasure or short travel (say, to get to and from work) can easily reach 600W – 800W for a short duration. The ability of the BEAU to keep pace with this level of power output makes the rider/motor combination capable of approaching elite cyclist sprint power outputs.

The goal of the BEAU is to allow a rider to either work less while traveling at their normal speed or travel at greater speeds under the same rider output power. Because the BEAU effectively doubles the rider's output this can easily be achieved. The BEAU has the ability to make a six degree incline at 16mph feel like a three degree incline at 15mph all while maintaining the feel of an unmodified bicycle.

---

### 1.3. GOALS OF THE BEAU

The BEAU's main goal is to be an attractively designed electric bike that is feature rich enough to be competitive in a market that is flooded with e-bikes ranging in quality and price. In order to reach this goal it must meet consumer needs and desires better than the competition.

1. **Completely Self-Contained.** For simplicity of both aesthetics and usability, the main goal of the BEAU is to be one object. In Smart Cities the concept of the robot-wheel, a wheel which contains as much of the drive mechanics as possible (in some cases even the steering drive as well), dominates the wheeled vehicle design process. For the BEAU, it is possible to contain all the mechanics, electronics, and sensors *inside* the rear wheel hub.

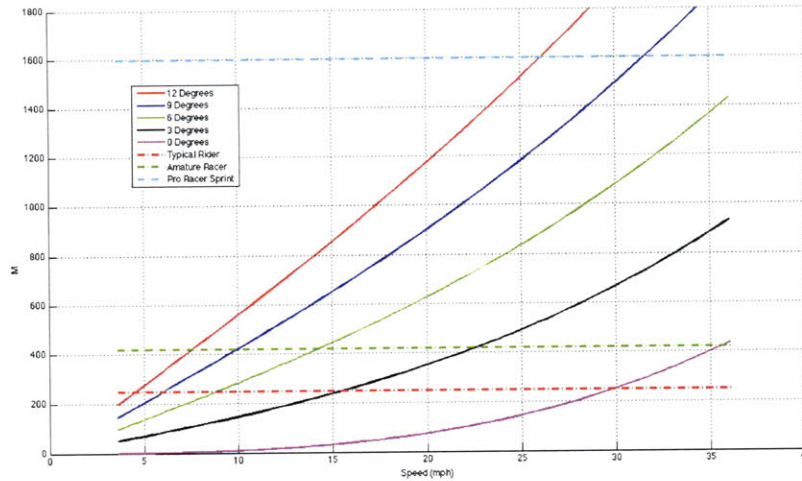


Figure 1.4: A graph of the motive power required versus speed for various slope angles.

2. **Modular Construction.** As a single unit the modularity of the BEAU is evident with respect to its ability to fit almost any bicycle. Inside the wheel-hub, the BEAU's components are arranged in a way that makes it easy to replace battery technology, circuit boards, and even the motor (given it fits the mounting constraints). It is important to try to find a balance between modularity and specificity. Just like programming, if code is too specific it becomes hard to use in other situations (see: polymorphism), but if it is too general your program tends to be very large and unfocused. In terms of the BEAU, the internal modularity has been abandoned in some cases in order to increase packing efficiency, but is still present.
3. **Aesthetically Pleasing.** Largely overlooked in engineering based design projects, it is very important that the BEAU be visually pleasing. Anodized aluminum exterior features that emphasize symmetry while keeping to the geometric form language of the bicycle are very important. Large, flat surfaces tend to make object like the BEAU wheel-hub look bigger than they are, while too many changes and breaks in the outer features lose the form of the whole.
4. **No Learning Curve.** The BEAU is intended to be a get on and ride type of device. One important reason for this goal is the Smart Cities group's dedication to the shared use model of vehicles where the vehicles are largely intended for public use. A vehicle that requires the user to learn new things to use is much less likely to be used than one that does not. Additionally, a vehicle that behaves like a bicycle will be easier to control than one that behaves like a scooter because all users who choose to rent a "bicycle" will already know how to ride one.





---

## 2.0. INDUSTRIAL AND PRODUCT DESIGN DESCRIPTION

The design of the BEAU follows the goals presented in Section 1.3. Using these goals, the design is guided by the engineering requirements of the components necessary to achieve the base goals. For example, the assembly order of the BEAU requires that the motor casing – which is also the outer casing of the BEAU – slide into place over the shaft. This dictates that the casing can only be attached with movement in the axial direction. Most optical encoders require an encoder wheel to be placed between a read-head and transmit-head. This cannot be accomplished with only movement in the axial direction and for this reason a magnetic encoder was necessary.

Much of the BEAU is guided in this manner. Starting from basic requirements a design for a product transitions into reality through careful consideration of the overall goals and the requirements of the components needed to accomplish those basic requirements. In order to discuss the overall design process of the BEAU (and any electromechanical system of this type), the path from a set of goals to a complete product is full of design, changes, and redesign. The result is the formation of a set of dependency trees that must be satisfied in order for the BEAU to work.

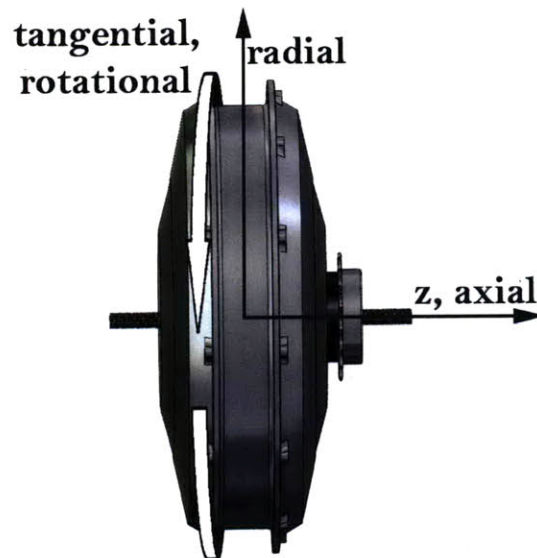


Figure 2.1: A diagram BEAU's outer casing as seen from the side. Directional indications are given for clarity of description in subsequent sections.

To begin, we will focus on the second design goal: modular construction. The requirement to fit

almost any bicycle affects the outer dimensions of the BEAU casing and the way the casing mounts to the wheel and the bicycle frame. Various bicycle rear fork spacings were measured in the field. It was found that most rear forks have a spacing of roughly 130mm. New bikes will have a fork spacing of 130mm to 135mm based on new standards for rear wheel spacing<sup>1</sup>. In order to fit almost any bicycle, the BEAU cannot be wider than 130mm, and should not be thinner than 100mm to avoid axial placement ambiguities and aesthetic problems.

The part of the BEAU design is most limiting in the width of the overall casing is the battery packs. The use of A123 Systems 26650 cells presents space limitations. These cells are nominally 26mm in diameter and 65mm long *without the paper non-conductive casing*. With the casing the cells are approximately 27.5mm in diameter and 66mm long. In reality the cells need to have connection points on the top and bottom, non-conductive packaging and a support structure. The over-all height (in the axial direction) of the battery pack and support structure is then increased to 70mm.

The sensors in the BEAU interface physically between the outer casing and the inner, non-rotating structure. For this reason the best and most obvious location for their placement is between the battery pack and the outer casing. This is true for the magnetic encoder which measures just the wheel velocity. The freewheel encoder measures wheel velocity plus freewheel velocity, and must be placed between the freewheel and the non-rotating structure (in this case, the motor shaft). On this side of the BEAU casing the flexure is placed roughly where the magnetic encoder is placed on the opposite side.

---

## 2.1. ENCODER PLACEMENT

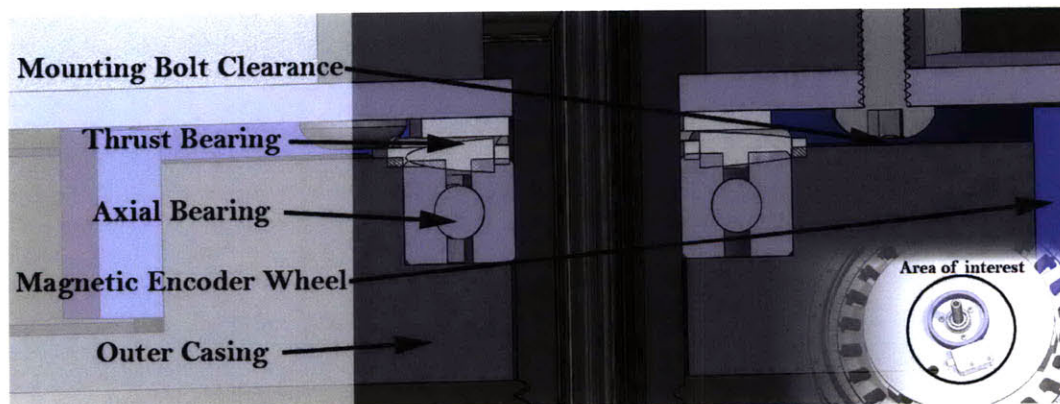


Figure 2.2: The magnetic encoder ring for the BEAU is read on the outer circumference by a magneto-resistive encoder that is similar in function to a hall-effect sensor.

---

<sup>1</sup>A standardized rear fork spacing makes it much easier for wheel/rim manufacturers to make wheels that fit every bicycle. In the past, a fork that was too small or large was simply bent into place by force.

### 2.1.1. THE MAGNETIC ENCODER

The magnetic encoder ring is press-fit onto the outer casing as can be seen in Figure 2.2. The combination of thrust and axial bearings serves as the main shaft support for this side of the casing and the axial support for the center structure. The clearance for the battery pack enclosure (not marked in the figure, but is the horizontal light blue-gray structure at the top of the image) bolts is very small, but is constrained by the width of the thrust bearing such that clearance issues are impossible despite the 0.40mm clearance.

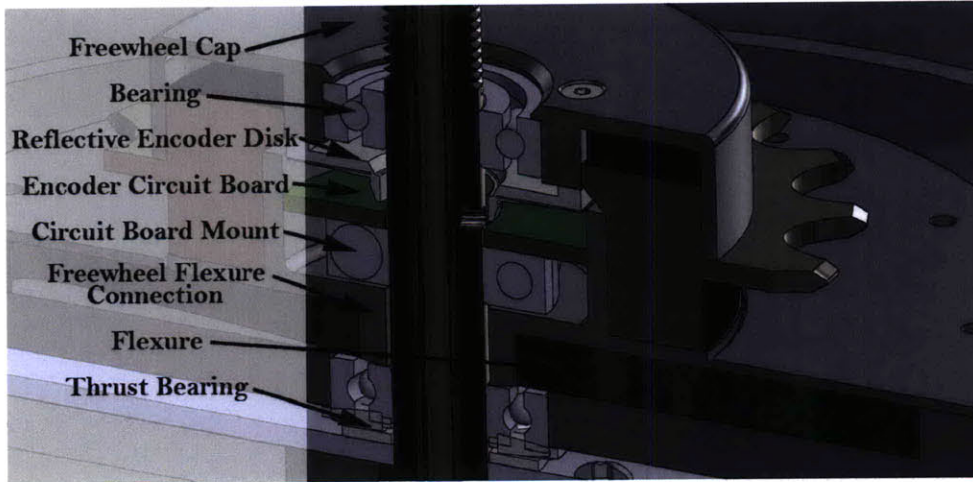


Figure 2.3: The reflective optical encoder is located inside the freewheel. The freewheel cap press-fits to the outer surface of the freewheel in order to actuate the freewheel encoder. The reflective encoder wheel is mounted to the freewheel cap.

### 2.1.2. THE OPTICAL ENCODER

The freewheel side of the outer hub is fairly complex in its assembly. The freewheel rotation is only accessible from the outer surface of the freewheel because the bearing takes up the entire width of the freewheel such that no internal surface rotates with the freewheel. For this reason the freewheel cap is necessary to move the rotation from the outside of the freewheel to the inside. The freewheel bearing is slightly wobbly. A wobbly connection to the reflective encoder wheel would lead to inaccurate readings. A bearing between the freewheel cap and the shaft (press-fit to the shaft) solves this issue by stabilizing both the freewheel and the reflective encoder wheel. Below the reflective encoder wheel the encoder read-head and counter ICs are located on the encoder PCB. This PCB is attached to a shaft collar that mounts to the main shaft. This allows for adjustment of the PCB position during assembly. The freewheel to flexure mount threads onto both the freewheel with a 1.370 x 26 TPI (english) thread and the flexure with a 16 X 1 (metric) thread<sup>2</sup>. The freewheel

<sup>2</sup>The mixing of units makes the author cringe, but while metric is preferred the freewheel is an english part where they are available easily. For reference several different thread sizes and pitches exist in both metric and english units for freewheels. This can be confusing at times.



to flexure mount must be made from steel because of the thin feature size and torque requirements of this piece. The flexure mounts directly to the freewheel-side outer casing. As with the magnetic encoder side of the outer hub, the combination axial and thrust bearing between the internal and external structures provide consistent support.

---

## 2.2. CASING TORQUE AND FORCE ANALYSIS

In terms of support and torque, the outer casing was designed to be as thin as possible. FEA analysis was performed on the casing in order to be sure of its structural integrity. The casing has a thickness at its thinnest of 3mm and is made from 6061 T6 aluminum. The analysis was performed with an applied torque of 50Nm and a downward force of 400N. The results show that the casing will not fail and has a safety factor of roughly 30.

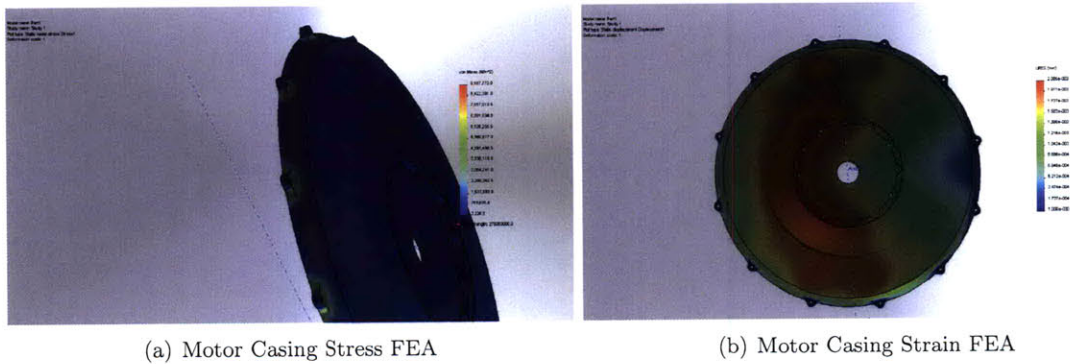


Figure 2.4: The motor casing FEA analysis shows that the casing will perform well under normal riding conditions. The stress safety factor is 30, placing it well below the yield criterion even for long term cyclic loading fatigue.

The strain analysis on the casing shows a maximum deflection of 0.002mm which is acceptable for the casing considering that it is also the motor casing which controls the air gap of the motor. When reviewing the strain diagram the reader will notice that the left half of the diagram is much more strained than the right. This is the result of the combination loading of torque and force on the casing. On the left side of the casing these forces add, and on the right side the torque is subtracted from the downward force (the direction is indicated by the vertical line in Figure 2.4(b)), resulting in a lower stress and strain on the right side of the casing than on the left.

---

## 2.3. INTERNAL ASSEMBLY

The internal assembly of the BEAU is the heart of the power, control, and support for the stator. The design requirements of the internal assembly include the following:

1. The internal assembly including the stator does not rotate
2. There must be enough room for at least 24 A123 26650 cells



3. The stator must be rigidly attached to the shaft in such a way that minimizes deflection
4. The Control circuitry should be placed in this area unless it is absolutely impossible to do so
5. The internal structure must be as thin as possible

Because the design of the motor dictated a certain diameter in order to meet the torque requirements of the design, the outer diameter of the internal assembly was well defined. In terms of supporting the stator, three supports is the minimum number of supports necessary to make the most of the support beam's strength. Two beams will suffer from greater beam deflection because they allow more cantilever deflection modes as opposed to compression and tension modes. The number of supports must be minimized in order to leave the most possible room for the battery packs. Because of the height of the battery packs and the fact that the beams did not need to use all of that height in order to provide rigid stator support, the main support beams are hollowed out in the center for the electronics of the BEAU.

The three battery bays easily fit 24 A123 26650 cells. Unfortunately they do not fit any more than 24 cells, but the extra room in the battery bays will allow for much needed wiring, packaging, and insulation space. As with any battery, these cells will tend to heat up as they are used heavily. The extra room in the battery bays will also serve to allow air to flow through the packs.

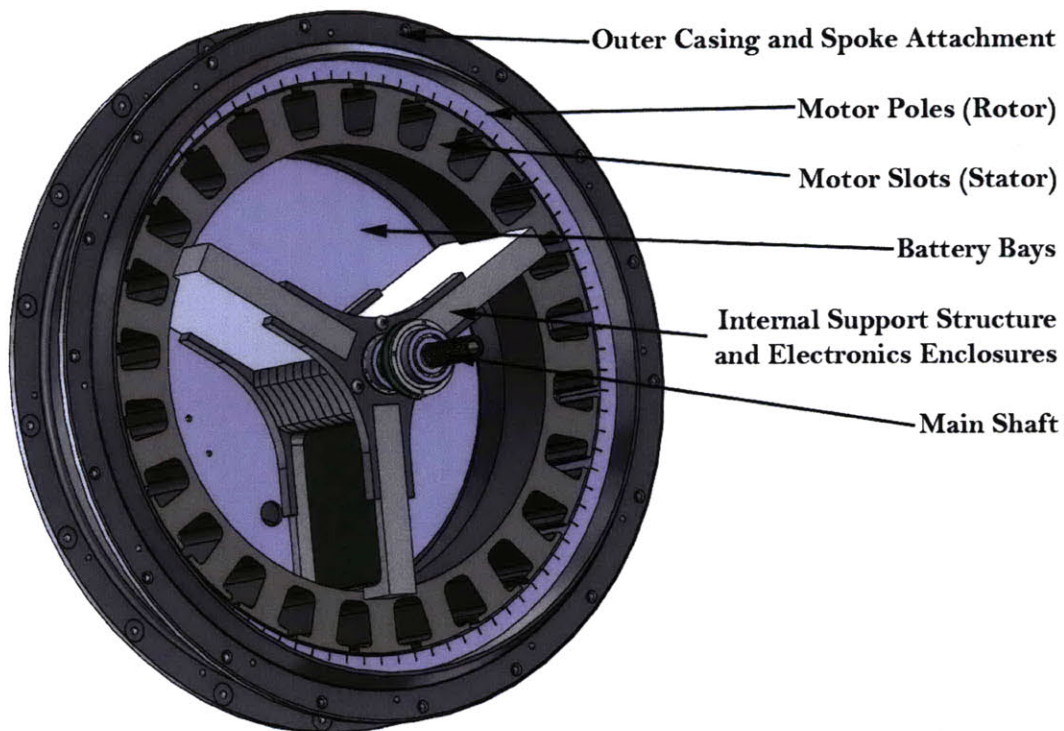


Figure 2.5: The internal layout of the BEAU. The A123 26650 cells are not pictured in this image.

The thickness of the internal structure is dictated by the height of the batteries. Care was taken in the design of this structure to allow for battery connections while minimizing the axial width of the battery pack. The two cover plates on either side of the pack (Pictured but not labeled. see “Battery Bays”) serve to secure the three beams to the central support structure that is attached to the shaft axially. These beams slide into the central support structure and are not bolted in place in any way. In the radial direction the beams are constrained between the stator and central support (notice the notch on the stator). The cover plates also provide axial mounting surfaces for the battery packs. Each plate is made from 1mm thick 6061 T6 aluminum.

As can be seen in Figure 2.5, the internal structure of the BEAU is relatively simple. Care was taken to make assembly and repair/troubleshooting an easy process by eliminating unnecessary bolts, screws, and mount points and instead taking advantage of already existing structures. For example, the battery packs rely on support from the stator support beams and the stator itself for positioning radial-tangentially. The center shaft mount (dark grey, centrally located supporting structure for the stator support beams in Figure 2.5), like the stator support beams, gets its axial positioning from the two cover plates that cap the internal structure.

In many previous figures where the main shaft has been pictured the reader may notice that it is hollow for a portion of its length on both sides. Previous instances of the BEAU concept have required opening the case or a hole in the outer casing in order to charge the batteries or reprogram the internal electronics. The BEAU attempts to solve this problem by making one side of the shaft a charging port and the other side a USB interface with the microprocessor.

The charging port uses the main shaft as ground and a large wire through the hole in the shaft as V+. The reason two wires were not run through the shaft is basically because they would not both fit, but using the main shaft as ground has the advantage of grounding the entire structure of the BEAU, which helps to prevent EM radiation leakage and accidental shocks. The charging pathways are required to be large because A123 cells are capable of charging at very high currents – making it possible to fully charge the BEAU in 10 - 15 minutes. This arrangement also makes the design of a “charging cap” that simply plugs into the end of the BEAU’s shaft easily and safely.

The USB interface on the opposite end of the shaft to the charging port allows for communication with the microprocessor through an Future Technology Devices International FT2232H dual UART USB interface IC. The ability to directly communicate with the microprocessor without having to remove the casing can be used to update the control code on the microprocessor during testing and control system verification. During normal use – as a product by non-technical user – the USB port can be used in combination with software on a computer in order to retrieve trip data and possibly change the assist ratio. Trip data includes data such as distance traveled, energy contributed by the rider, energy used by the motor, and velocity versus trip progress graphs.

---

#### 2.4. AESTHETICS

Aesthetics, in the interest of this document, is defined as the industrial engineering side of the design of the BEAU. To many it is considered an art – a subjective process that results in subjective appearance. Because of this conception industrial design is much harder to quantify and evaluate

than product design, which is based in engineering and hard numbers<sup>3</sup>. Industrial design seeks to elicit a feeling from the viewer. This feeling is in the form of an idea or emotion that does not necessarily require expression in words. It is the goal of the designer to make the evocation of his work as universal as possible – walking the line of objective emotion.

The BEAU has a fair challenge in the aesthetics department because it is only a small part of a largely undefined overall look. That is, the bicycle to which the BEAU attaches is unknown. In order to maintain a consistent form language throughout, care must be taken to recognize and characterize the idea of the bike as a form of its own and make the lines on the BEAU's outer casing reflect that form.

The BEAU does not have a lot of room for changes to its form. It must be cylindrical in nature for rotational symmetry reasons – otherwise it would wobble instead of spin! The width of the casing at its attachment point to the bicycle is fairly well defined and must fall within the 120mm to 130mm range. Even the diameter of the casing is defined by the motor and the necessity to minimize spinning mass – this means that the outer diameter must be just larger than the outer diameter of the motor rotor.

So what can be changed? The BEAU casing transitions from 30mm in thickness to 121.69 mm in thickness from its outer edge to the shaft mount point. The profile of this transition is what can be changed. The profile could be made to be a spline, a smoothly varying curve throughout the radius of the casing; a tangential curve, angular surfaces whose transitions are smoothed by tangency curves; or an angular surface, flat surfaces with angular intersections and no curved transitions.

Initially, one might perceive the bicycle as having the form language of curves. Its frame is generally made with cylindrical tubing, round wheels, and circular motion of the pedals and wheels. In fact this is not the case. If asked to draw a bicycle most would respond by drawing hard angular lines in triangular shapes with circles for wheels. The form of the bicycle is actually angular in nature.

For this reason the BEAU is designed using angular features as can be seen most easily in Figure 2.1. The profile abruptly increases to allow room for the internal components, then slowly transitions to full width. The break between the transition serves to reduce the perceived diameter of the casing. Without this break the entire surface would look more like a featureless flat plate.

---

<sup>3</sup>...or so the conception goes. The author would like to argue that industrial design is less subjective and product design is more subjective than perception suggests.



---

## 3.0. THE MOTOR: MOVING THE BEAU FORWARD

The BEAU uses a custom 800W peak, 24-pole, three-phase, frameless, brushless DC torque motor. In the electric bicycle world this type of motor is used occasionally with the best example of its use in the BionX electric bicycle conversion kit. This type of motor is available commercially, but limitations on budget and size options required the motor to be custom designed. This section will cover a small amount of the basics of motor design, the specific design of the BEAU's motor, and the BEAU motor fabrication process.

---

### 3.1. MOTOR DESIGN BASICS

Brushless motors differ from brushed motor in the fact that – as their name suggests – they do not have brushes. The brushes in brushed motors serve the purpose of controlling the commutation of the motor. That means that the brushes determine which coils on the motor get energized depending on the rotational orientation ( $\theta$ ) of the motor. Brushless motors require electronic commutation. In general, both brushed and brushless motors are built the same way in terms of the arrangement of magnets and coils, which varies greatly depending on the purpose and requirements of the motor.

A motor is a magnet machine that uses electric current to produce kinetic or mechanical energy through electromagnetic force. The electric motor was first invented by Michael Faraday in 1821. It consisted of a free-hanging wire that was hung like a pendulum in a pool of mercury. The center of the pool contained a magnet. When an electric current was run through the wire it rotated around the magnet. Faraday made a simple magnetic circuit in order to cause a physical rotation.

#### 3.1.1. AIR GAP FLUX DENSITY

A magnetic circuit is made of one or more closed loop of magnetic flux. Magnetic circuit analysis exploits the relationships between the equations that describe magnetism and magnetic flux and those that describe electricity and electrical circuits. Using these circuits we can develop ideas about how a motor works and use these ideas to aid in its design.

Figure 3.1 shows the flux path for one loop of the BEAU's motor. This loop repeats for every half-pole pair in the motor. For the BEAU's motor which has 24 poles this means that there are 24 half-pole loops. In order to transform this diagram of the flux path into something that mathematically and scientifically understood, we will use the theory of magnetic circuits. Through the path of flux there are resistances to and sources of flux. The air gap between the rotor and stator, for example, is a very large resistance to flux. The total flux crossing the air gap is the sum to the coil and permanent magnet flux, or  $\Psi_T = \Psi_r + \Psi_c$ .

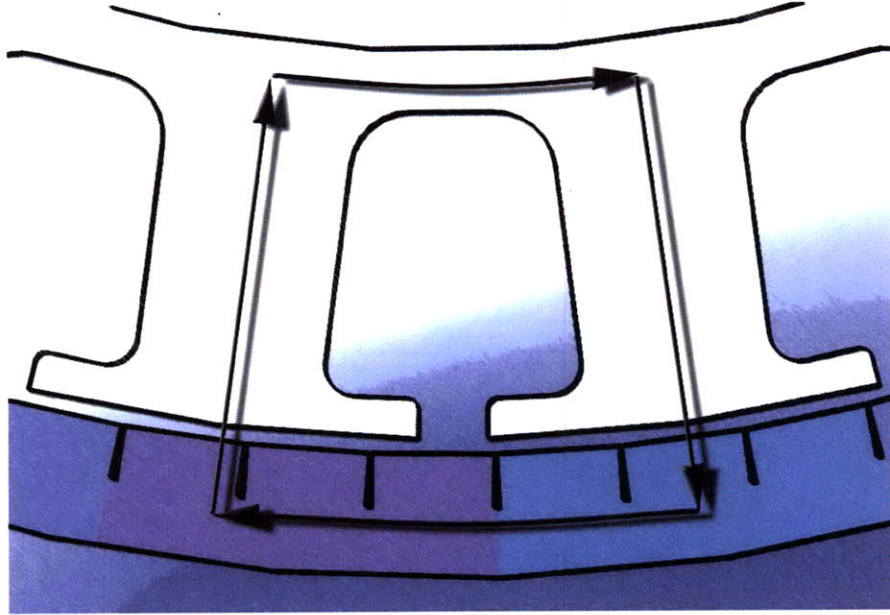


Figure 3.1: A diagram of the flux path for one loop in the BEAU's motor.

The magnetic circuit model shown in Figure 3.2 has two values for the reluctances of the rotor and stator. The first value ignores flux leakage between elements (such as leakage between the magnets that does not pass through the stator) and the second takes them into account. From Hanselman [7] we can see that

$$R_m = \frac{l_m}{\mu_0 \mu_R A_m} \quad (3.1)$$

$$R_g = \frac{g}{\mu_0 A_g} \quad (3.2)$$

where  $l_m$  is the motor length (depth),  $\mu_0$  is the vacuum permeability,  $\mu_R$  is the recoil permeability<sup>1</sup>,  $A_m$  is the cross-sectional magnet area,  $g$  is the air gap distance, and  $A_g$  is the cross-sectional air gap area. In order to account for flux leakage and reluctance variability in a simplified manner we will use the constants  $K_l$  and  $K_r$  for flux leakage and reluctance variability respectively. This gives an air gap flux of

$$\Psi_g = \frac{K_l}{1 + K_r \frac{\mu_R g A_m}{R_m A_g}} \quad (3.3)$$

Combining Equations (3.1), (3.2), and (3.3) with the air gap flux density definition –  $B_g = \frac{\Psi_g}{A_g}$  – gives a good estimation of the flux density of a motor based on elementary physical constants such

<sup>1</sup>Recoil permeability is an indication of a permanent magnet's ability to magnetize and demagnetize. In terms of the magnetic hysteresis loop, it is equal to  $\frac{dB}{dH}$  on a B-H plane for a given magnetic material[12].

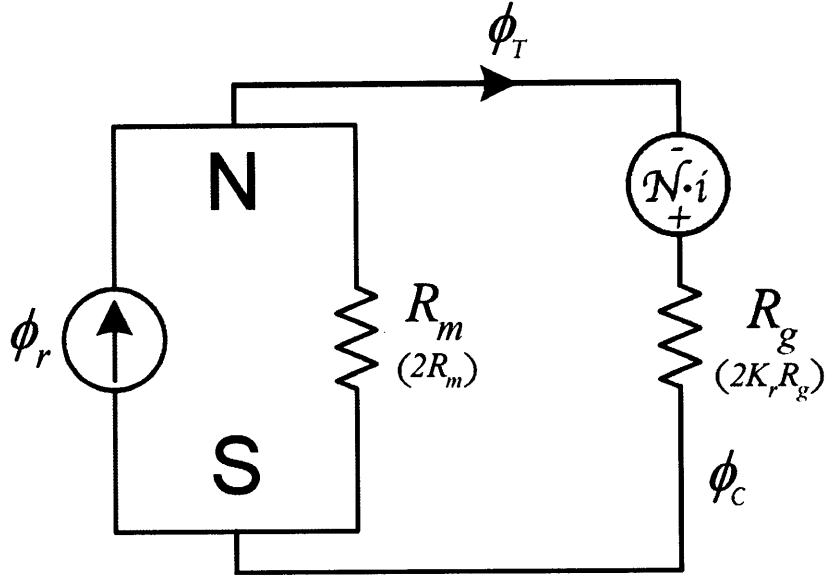


Figure 3.2: A diagram of the magnetic circuit for the close loop flux path.

as the air gap and magnet length and cross-sectional area.

$$B_g = \frac{K_l C_\Psi}{1 + K_r \frac{\mu_r}{P_c}} B_r \quad (3.4)$$

$C_\Psi$  is equal to  $\frac{A_m}{A_g}$ ,  $P_c$  is equal to  $\frac{l_m}{g C_\Psi}$ , and  $B_r$  is the flux density of the magnet. In terms of motor design, we can see that it is important to keep the air gap area equal to the magnet area. This can be accomplished by designing the heads of the stator to be roughly the size of the magnets per pole[1]. The air gap distance is the key value that can be changed to modify the resulting motor torque.

### 3.1.2. MOTOR TORQUE

The flux density across the air gap is the driving factor in motor motion; it represents the energy gradient between the rotor and stator. Together with  $N$ ,  $r$ , and  $l_s$  the flux density forms the motor constant[13]. The resulting motor torque can be reasonably approximated with

$$\tau = (4NB_g l_s r) i, \quad (3.5)$$

which is the torque produced by a single phase of a brushless motor<sup>2</sup>.  $N$  is the number of turns *per phase*,  $l_s$  is the stator length (in the z direction, parallel to the motor's axis of rotation), and  $i$  is the current supplied to the coils. The parenthesis are to indicate the part of Equation (3.5) that

<sup>2</sup>This equation also works for brushed motors

form the motor torque constant, or  $K_t$ . The constant '4' is determined through the drive technique (trapezoidal) and the number of passes through the EM field per loop (2)<sup>3</sup>.

---

### 3.2. MOTOR CALCULATIONS AND FEA ANALYSIS FOR THE BEAU

For calculations we will use:

- $K_t = 1$
- $K_r = 1.1$
- $C_\Psi = 1$
- $\mu_R = 1.05$
- $P_c = 3$
- $B_r = 1.38$  Teslas for N48 grade neodymium
- $N = 20$  turns
- $B_g = 0.996$  Teslas
- $l_s = 0.030$  meters
- $r = 0.115$  meters
- $i = 0 \rightarrow 20$  amps

Calculations yield a flux density in the air gap ( $B_g$ ) of 0.996 Teslas. Using this value we can see that the torque output per pole is  $K_{tpole} = 0.275 \frac{Nm}{A}$ . Each phase has 8 poles ( $\frac{24poles}{3phases}$ ), and two phases are driven at one time in a WYE winding configuration, which gives us  $K_{tmotor} = 4.40 \frac{Nm}{A}$ . At peak torque the BEAU motor should be able to output roughly 85Nm.

#### 3.2.1. FEA RESULTS - GRAPHS

In order to speed up the design process the motor for the BEAU was modeled using math only to the point of determining relative size, number of poles, winding requirements, and air gap. The rest of the design process was completed with the help of motor magnetic FEA software called MotorSolve. The software allows a motor to be evaluated accurately and quickly, providing feedback such as non-idealized torque curves, back EMF, magnetic saturation, and motor efficiency.

#### TOTAL TORQUE VERSUS ROTATIONAL VELOCITY

Figure 3.3 shows the torque output of the motor versus rotational speed. The FEA predictions and the theoretical predictions of the maximum torque in the magnetic circuit model are very close.

---

<sup>3</sup>For sinusoidal drive, this constant should be 3. Also this definition of torque is for approximation only and will usually only be within a factor of two of the actual motor output torque. This accuracy is reasonable because it allows a motor designer to quickly ballpark a motor and the required drive techniques.



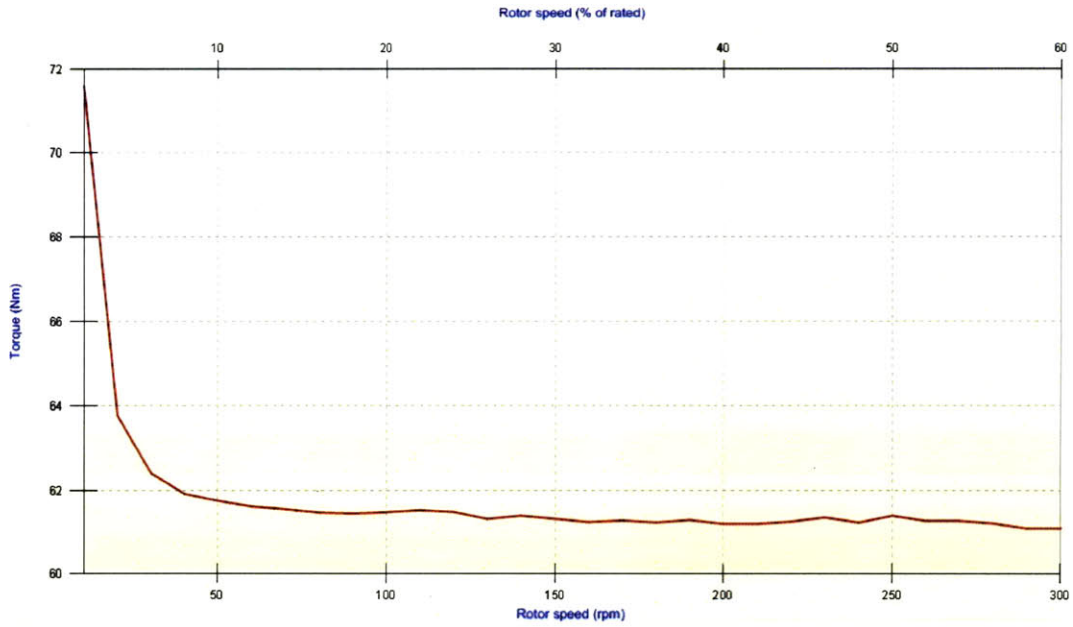


Figure 3.3: The total predicted torque output of the BEAU's motor.

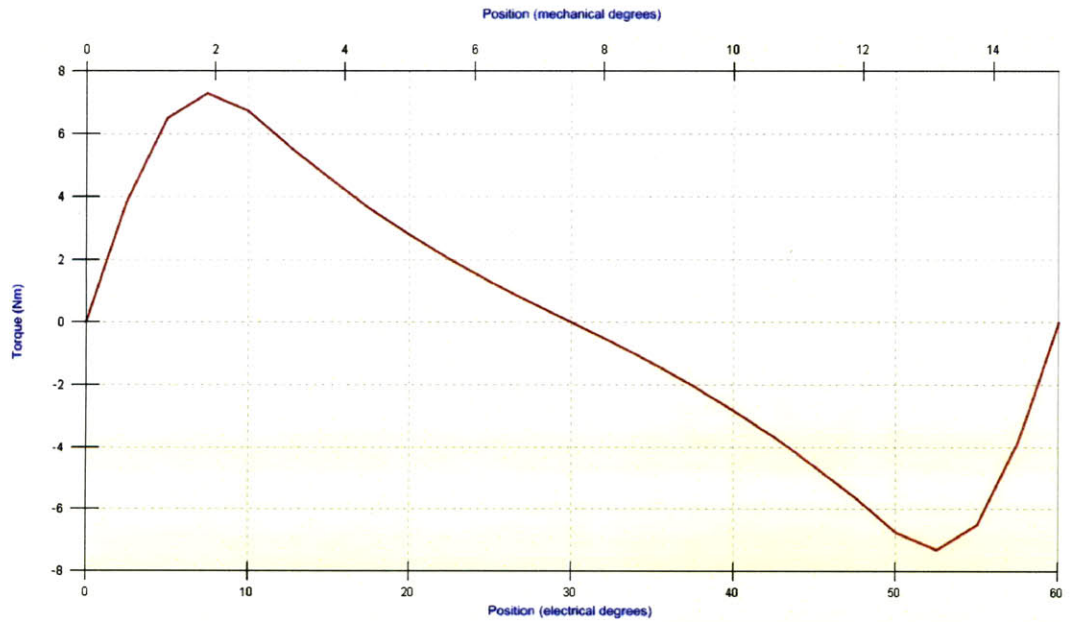


Figure 3.4: The phase angle dependent cogging torque of the motor.

This result confirms the motor design and allows the design to move to manufacturing with the confidence that a working motor that meets the require specifications will result. Below are other

relevant outputs of the motor FEA software. Of interest is the plot of flux density over the surface of the motor.

### COGGING TORQUE VERSUS PHASE ANGLE

We can see from figure 3.4 that the cogging torque is at maximum 7Nm. This is slightly high for the motor during “motor off” scenarios, but will be acceptable during motoring. In order to reduce this force the motor armature can be skewed. Skewing rotates the laminations axially as they are stacked, effectively smoothing out the transition between one pole and the next. Analysis with the MotorSolve software shows a decrease to 4.5Nm cogging torque with a 5 degree skewing angle[14].

### BACK EMF VERSUS PHASE ANGLE

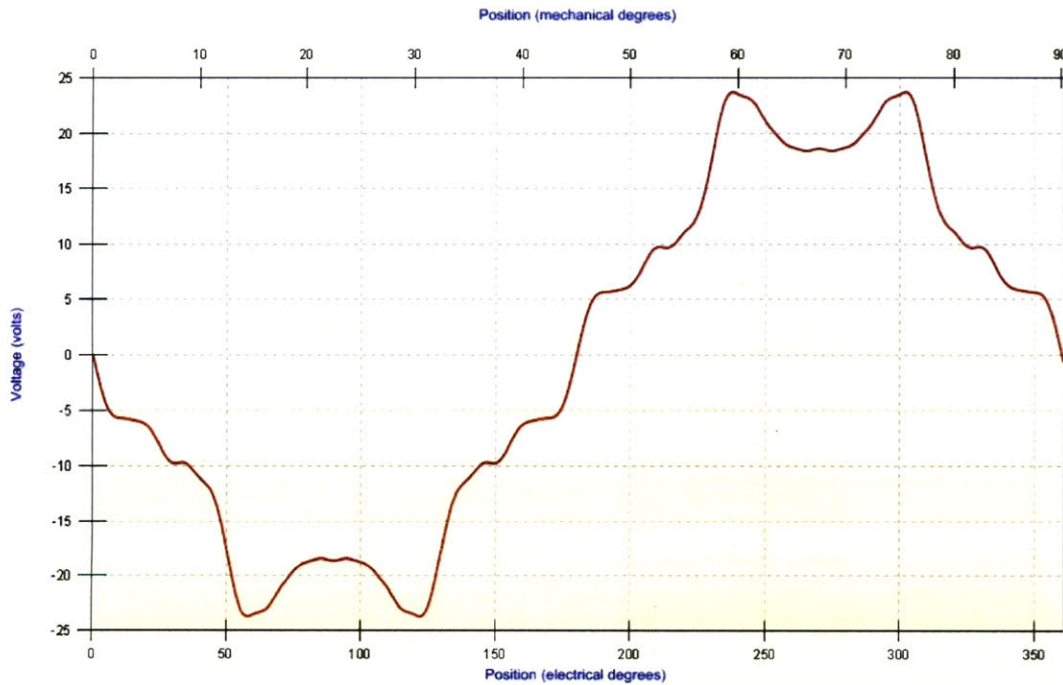


Figure 3.5: The back electromotive force produced by the motor.

The back-EMF of the motor is used to gauge the rotor’s electrical position. Back-EMF is also the reason why a motor has a maximum speed even while completely unloaded. Back-EMF generation is a function of  $\omega_{motor}$ , generally presented as  $e_{bemf}\omega_{motor}$  where  $e_{bemf}$  is the back-EMF constant for the motor or phase.

Prototype Design 1

Flux function  
Flux density

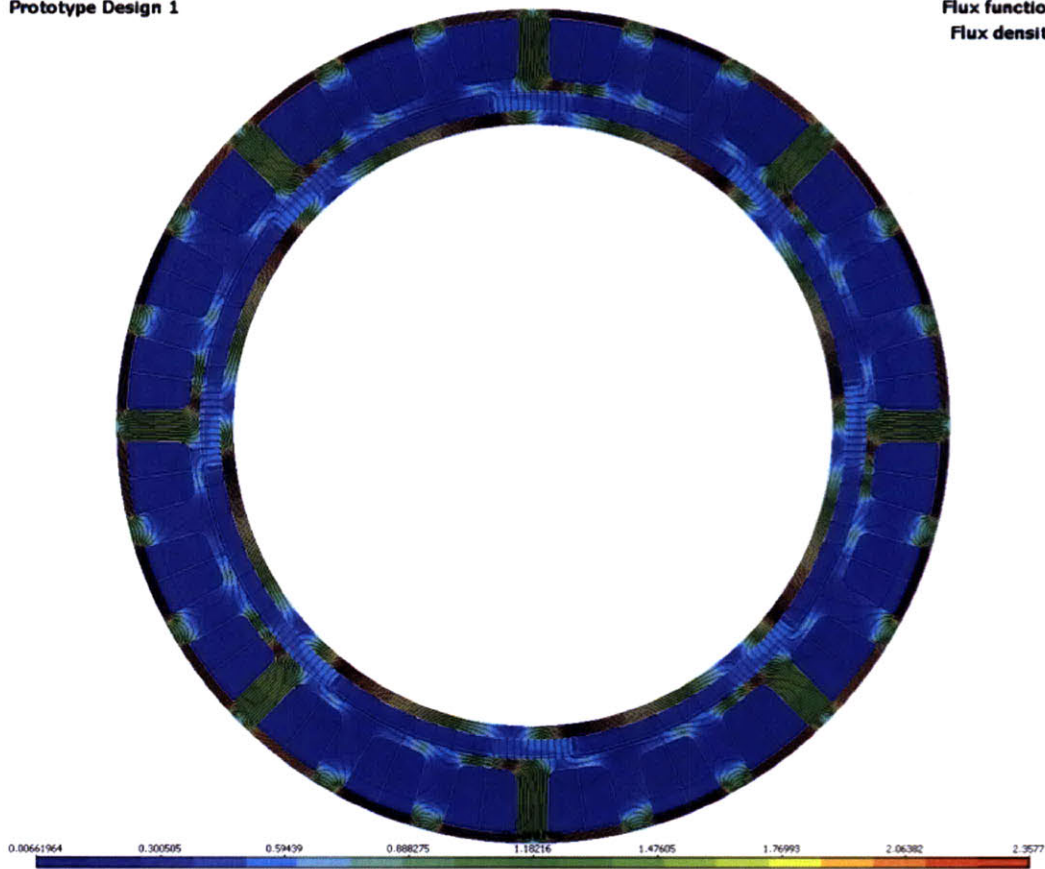


Figure 3.6: An indication of the flux density distribution throughout the motor.

### 3.2.2. FEA RESULTS - PLOTS

#### FLUX DENSITY

The flux density plot helps determine areas of potential flux saturation. Flux saturation means that a conductor of flux has reached its maximum capacity. Like a wire conducting current, flux capacity is based on conductor physical dimensions and material. Unlike a wire conducting current, flux saturation does not result in fire.

TOTAL POWER LOSS

Prototype Design 1

Total loss

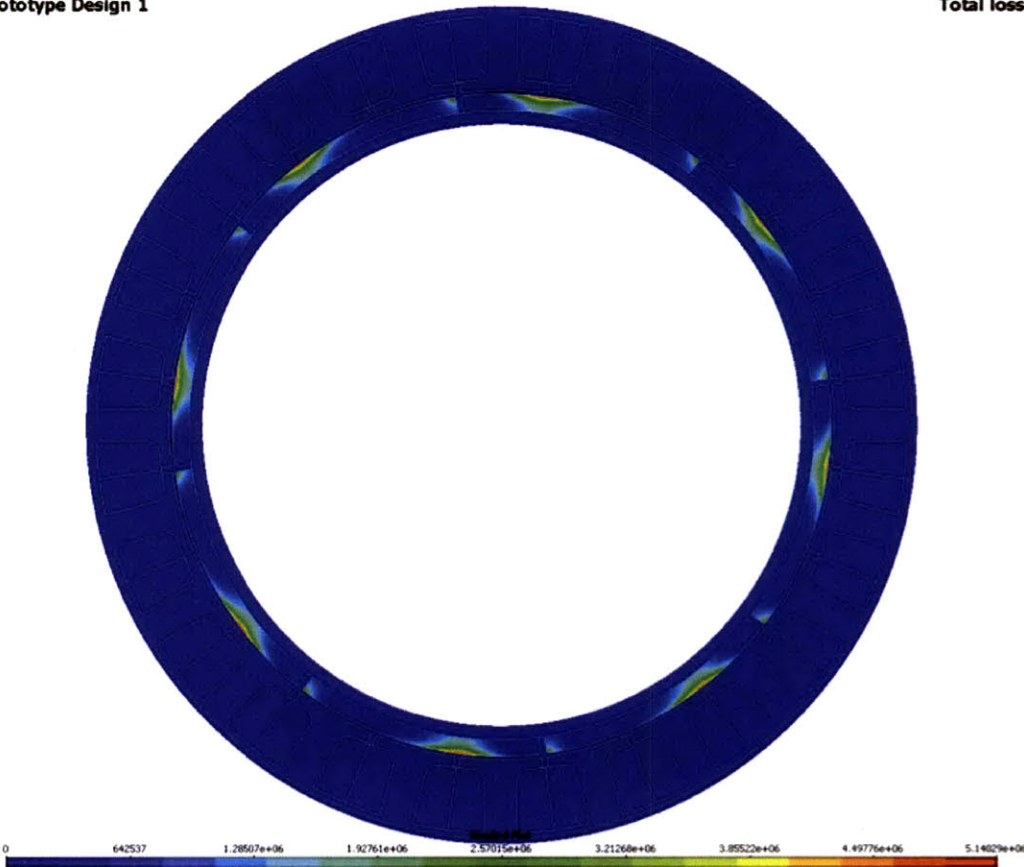


Figure 3.7: A diagram of the total energy loss during operation and where it occurs.

---

## 4.0. THE CONTROL APPROACH, THEORY AND IMPLEMENTATION

This chapter will cover the basic theory behind the control of the BEAU from a control theory perspective with relevant detail given to the physical motor and vehicle dynamics and the electrical characteristics of the motor and control system. The control is implemented on a custom electronic circuit built for the BEAU. The circuit implements an Atmel based microcontroller and an Allegro Micro based MOSFET driver for power switching.

The BEAU relies on input from the rider to direct the motor's output power via current control. The rider input is in the form of a torque parameter that is measured using a flexure-based torque sensor, the design of which is described in Chapter 5. The torque input is combined with the wheel velocity to determine the total power that the user is providing to the system. This power can be equated into the electrical regime by dividing it by the voltage of the supply, yielding a current input for the motor modified by known motor inefficiencies.

---

### 4.1. CONTROL APPROACH

The BEAU control system is intended to be completely devoid of conscious input by the user. In other words, the user should not have to think about control strategies while riding a BEAU enabled bicycle. In order to accomplish this the method of determining the desired motor torque must be based on a parameter that can be measured without modifying the normal user interaction with a bicycle. It becomes obvious from this design goal that the best way to control the motor is to base its torque on the torque provided by the user during travel. There are various ways of accomplishing this:

1. Force sensors on the pedals: using force sensors on the pedals will give an indication of the contact force between the riders feet and the pedals at any given time. This force can be translated into torque at the wheel by multiplying by the pedal radius, dividing by the first sprocket radius, and multiplying by the wheel sprocket (freewheel) radius. This sensor would need to be on a rotating part of the bicycle<sup>1</sup>
2. A torque sensor on the drive sprocket: This is one of the most common placements for torque sensors on bicycles. The torque sensor is located in the connection between the drive sprocket and the frame (the drive sprocket is connected directly to the pedals). This allows torque sensing without requiring the sensors to be rotating.

---

<sup>1</sup>“This sensor would need to be on a rotating part of the bicycle.” is a nod to the fact that in most cases the processing electronics would be on a part of the bicycle that would *not* be rotating. This brings about several issues that necessitate the use of slip-rings or RF circuits to resolve.

3. A chain-based resonance measure of torque: Based on elementary kinematics theory, the vibration frequency of the chain is an accurate measure of the tension on the chain. If this frequency is measured using inductive or capacitive sensing, the torque on the chain can be approximated. This is an academically interesting yet difficult to implement solution to measuring torque.
4. Strain-gauge based torque sensors in the motor casing: Because the motor casing only experiences the motor's torque at the outer edges of the casing, it is possible to place strain gauges on the casing between the freewheel connection and the wheel mount to measure the strain, and therefore torque, on the casing due to the rider input. This would require the sensors to be rotating.
5. Flexure based torque measurement: By placing a spring between the freewheel and the motor casing, the torque can be directly sampled as a function of spring displacement. This has several advantages due to the fairly linear torque-displacement curve of a flexure under load. This would require that the sensor be rotating<sup>2</sup>.

#### 4.1.1. TORQUE SENSOR SELECTION

A major design goal of the BEAU is that it be completely self-contained. Taking this into account, it is obvious that all but the last two options in the above list are not applicable. Item 4 is a valid option, but the necessity of slip rings or RF devices in order to communicate the strain measurement to the internal non-rotating electronics make this option less preferable because RF is likely to be difficult due to interference with the motor RF emissions and slip rings are inherently noisy and large. Item 5, the flexure based torque measurement, is likely the best option for several reasons. Not only does it provide a clean torque estimate over the entire range of possible torque input from the user, it also provides a spring constant between the freewheel and the wheel, which acts to decrease the slope of the line on which the motor torque output needs to reside[4].

The graph in Figure 4.1 shows the torque contribution of the motor with reference to the wheel velocity given a fixed velocity input provided by the user. Keep in mind that this is *not* the total torque output of the motor, merely the effective torque output to the ground after factoring in the torque provided by the user to maintain the wheel at the fixed velocity input. Also, the graph represents the instantaneous state where the motor meets a specified torque requirement. After this point in time the wheel velocity will increase due to the motor's effective torque contribution being non-zero, which will move the fixed velocity to a new point.

If the motor's torque is not high enough to reach the wheel velocity of the rider, then the motor will effectively drag on the user, the curve is effectively flat in this region, but in reality it has some small non-zero slope. At the point where the motor's torque is equal to the rider's input torque the motor begins to contribute to the system. This part of the curve is very steep because a very small amount of torque increase from this point will lead to the motor outpacing the rider, causing the rider's drivetrain to freewheel, and effectively leading to the rider contributing zero torque to the system. The spring in the flexure helps to control this situation by providing a direct sensor link between position on this steep slope and motor torque.

---

<sup>2</sup>In this case, this rotation can be abstracted away from the problem by using differential optical position encoders.



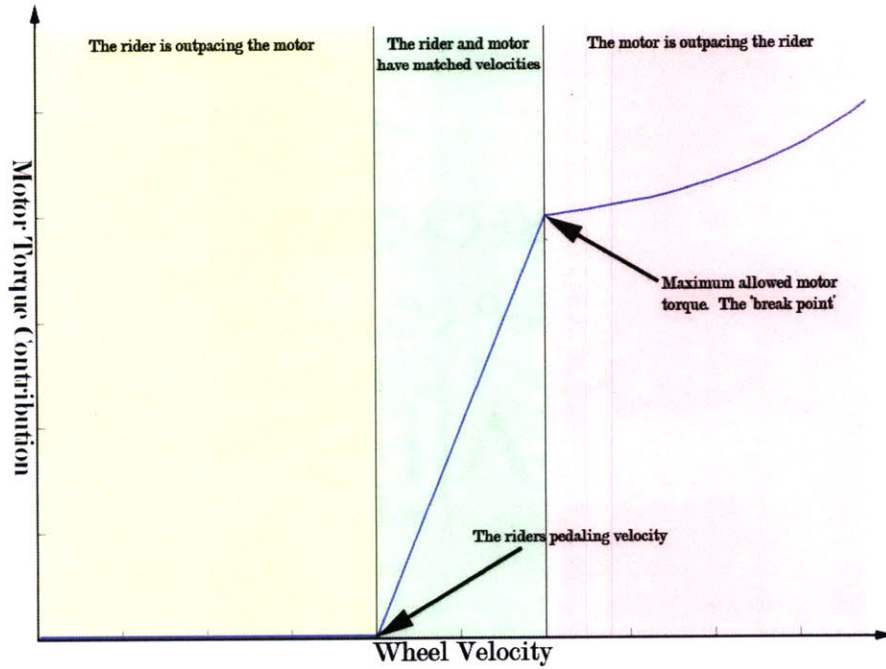


Figure 4.1: From the motor’s perspective, the torque construction must match the riders velocity while providing torque in a range that neither drags on the user nor overpowers the user. Unfortunately this zone (in green) has a very steep slope. The spring in the flexure helps to lessen the slope while also accurately instrumenting it in order to provide precise feedback to the control system.

#### 4.1.2. SYSTEM DYNAMICS

The BEAU is meant to control the system that includes not just itself, and the rotational inertia of its casing and the input torque of the rider<sup>3</sup>, but also the *unknown* rotational inertia of the wheel, the linear inertia of the bicycle and its rider.

During periods of motoring, the motor will be controlled with a second-order proportional-differential position controller. The position in question is the displacement  $\theta_{flexure}$ , which translates directly to the error of  $\theta_{pedal} - \theta_{wheel}$ <sup>4</sup>. The control system will seek to make  $\theta_{pedal} - \theta_{wheel}$  zero at all times. With reference to Figure 4.1 we can see that this will create a situation where the motor torque is always equal to the rider’s input torque.

The BEAU will not always be motoring. During times when  $\theta_{pedal} < \theta_{wheel}$  but  $\theta_{pedal} > 0$  (both  $\theta_{pedal}$  and  $\theta_{wheel}$  are referenced from the bicycle shaft, which is rigidly attached to the bicycle frame) the BEAU will be in “coast” mode. In this mode the motor will be electrically off, allowing

<sup>3</sup>Keep in mind that this torque input is a kinematic input to the control system that is connected to the wheel through a spring. The control system must act in such a way as to keep this spring under minimum deflection.

<sup>4</sup>There is interchangeability between  $\theta_{wheel}$  and  $\theta_{motor}$  because the two are mechanical identical measurements.  $\theta_{pedal}$  is the measurement of the freewheel itself, which is not only connected to the motor via the spring flexure, but also is allowed to freewheel when  $\theta_{pedal} < \theta_{wheel}$ .

the bicycle to coast as a normal bicycle would. During times when  $\theta_{pedal} < 0$ , (The rider is pedaling backwards) the BEAU will enter regenerative braking mode, slowing the bicycle down proportionally to the speed at which the rider is pedaling backwards. This regenerative braking technique allows the normal physical breaks to function nominally. Figure 4.2 shows the overall topology of the BEAU's control system.

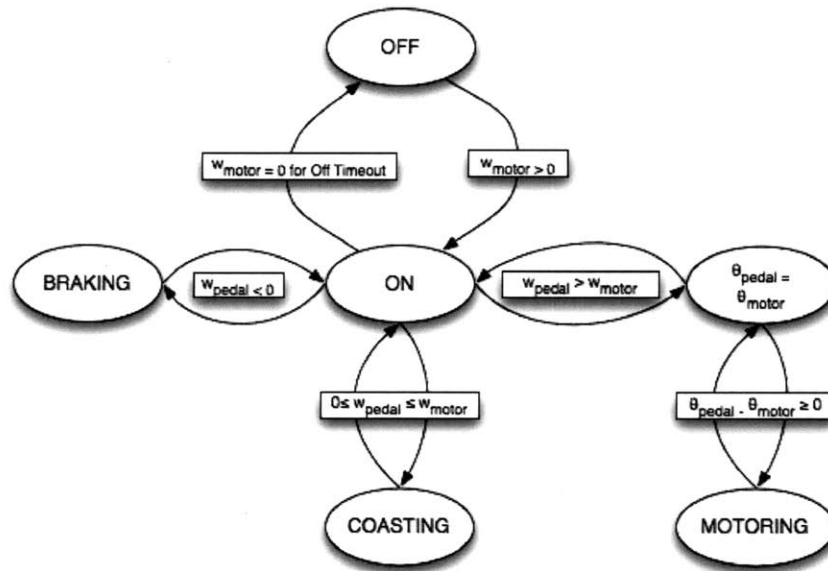


Figure 4.2: A diagram of the various states in which the BEAU can exist during operation. Note that the off and on states are triggered automatically and require no conscious user input.

---

## 4.2. CONTROL IMPLEMENTATION

Many of the standard control system techniques are very familiar. The BEAU does not use any out-of-the-ordinary control scheme. The BEAU implements a simple PD controller which transforms between  $\theta$ -space and voltage space in the form of an adjustable resolution PWM output signal[2]. For the purposes of simulation the PWM constants can be removed in order for the controller to interact with the plant model more easily.



#### 4.2.1. THE ELECTRICAL EQUATIONS

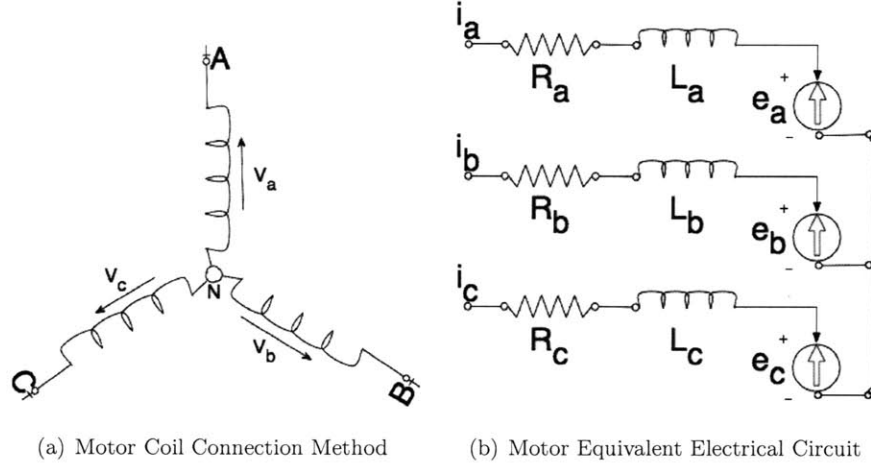


Figure 4.3: Diagrams of the motor electrical systems. The motor is wound with a WYE type winding as opposed to delta. The equivalent circuit used to calculate the plant model in the control systems tests.

The motor's design makes it a very large inductor. This inductance tends to oppose changes in current. The motor also generates a back-EMF voltage which is based on  $K_E$  and  $\omega_m$  (the back-EMF constant and the angular motor velocity), and resists the flow of current with a resistance  $R$ [18]. Ignoring the three separate phases of the motor we can show that the voltage in terms of  $i$  and  $\omega_m$  is

$$V = L \frac{di}{dt} + Ri + K_E \omega_m. \quad (4.1)$$

In order to get the phase specific solutions the number of pole pairs comes into play[5]. For a three-phase, thirty-two pole motor the number of pole pairs is 16. This number is multiplied by  $\theta_{motor}$  in order to get the electrical phase angle, or  $\alpha = p\theta_m$ . With the electrical phase angle known we can determine the voltages for each phase.

$$\begin{aligned} V_a &= i_a r + L \frac{di_a}{dt} + K_e \frac{d\theta_m}{dt} \sin(\alpha) \\ V_b &= i_b r + L \frac{di_b}{dt} + K_e \frac{d\theta_m}{dt} \sin\left(\alpha + \frac{2\pi}{3}\right) \\ V_c &= i_c r + L \frac{di_c}{dt} + K_e \frac{d\theta_m}{dt} \sin\left(\alpha + \frac{4\pi}{3}\right) \end{aligned} \quad (4.2)$$

For current, the same holds.

$$\begin{aligned}
 i_a &= i_t \sin(\alpha) \\
 i_b &= i_t \sin\left(\alpha + \frac{2\pi}{3}\right) \\
 i_c &= i_t \sin\left(\alpha + \frac{4\pi}{3}\right)
 \end{aligned} \tag{4.3}$$

#### 4.2.2. THE DYNAMIC EQUATIONS

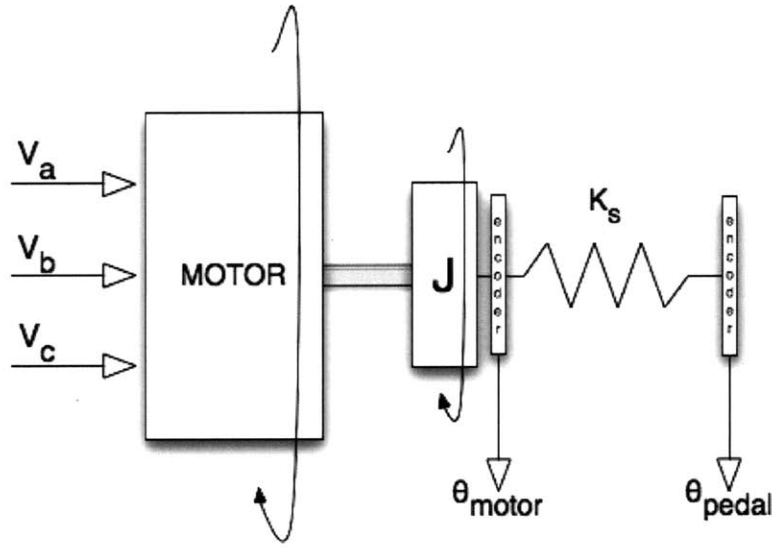


Figure 4.4: A dynamic model of the BEAU in a simple form. All inertial terms can be lumped.

Figure 4.4 shows a simplified representation of the motor and overall system's physical dynamics. The dynamic equations are slightly more difficult to simulate because the mass of the bicycle, rider, and wheel are not known (nor will they ever be), but these uncertainties can be addressed through the controller and are therefore not necessary to consider these varying parameters while developing the plant model because the range of the unknown's possible values are known.  $\tau_m$  can be determined from physical parameters to be

$$\tau_m = K_t i = (J_m + J_w + r^3(m_B + m_r)) \frac{d^2 \theta_{motor}}{dt^2} + f \frac{d \theta_{motor}}{dt} - K_s (\theta_{pedal} - \theta_{motor}). \tag{4.4}$$

Combining Equations 4.2, 4.3, and 4.4 allows us to reach a plant model[20]. The plant is referred to as an equation in the s-domain that is a quotient of the output variables over the input variables for a given system, thereby simulating the physical response of a real system through the use of analysis. In implementation, the plant equations do not exist in the microcontroller.

### 4.2.3. THE CLOSED-LOOP CONTROLLER

The plant can be modeled in terms of the motor constant  $K_m$  and the torque constant  $T_m$ . The electrical torque constant  $T_e$  can be shown to be much smaller than  $T_m$  and can thus be neglected in the plant modeling[6]. For any plant analysis and feedback response presented in subsequent sections it is the goal of the author to approximate correct values for the proportional and differential gains in the system in order to save physical calibration time as well as confirm understanding of the system. The  $G(s)$  transfer function for the plant is simplified to

$$G(s) = \frac{K_m}{s(sT_m + 1)}. \quad (4.5)$$

This transfer function takes a voltage input and gives a theta ( $\theta_{motor}$ ) output for completion of the control loop. For simulation the voltage request to PWM<sup>5</sup> request transformation was left out of the controller<sup>6</sup>. For a simple PD controller, we can see that the transfer function must be

$$C(s) = \frac{K_{PWM}}{V_{batt}}(1 + K_d s)K_p \theta_{err}, \quad (4.6)$$

where  $\frac{K_{PWM}}{V_{batt}}$  is a constant of units  $\frac{1}{voltage}$  which converts the voltage request of the controller into a PWM duty cycle request that the microprocessor can use to control the MOSFET drive IC. In reality it is necessary to control all three phases with separate PWM requests. For trapezoidal control, the three controller equations are simply Equation 4.6 modulated by the phase (a, b, or c) and that phase's phase angle in the continuous domain.

$$\begin{aligned} C_a(s) &= \frac{K_{PWM}}{V_{batt}}(1 + K_d s)K_p \theta_{err} \sin(\alpha) \\ C_b(s) &= \frac{K_{PWM}}{V_{batt}}(1 + K_d s)K_p \theta_{err} \sin(\alpha + \frac{2\pi}{3}) \\ C_c(s) &= \frac{K_{PWM}}{V_{batt}}(1 + K_d s)K_p \theta_{err} \sin(\alpha + \frac{4\pi}{3}) \end{aligned} \quad (4.7)$$

Simulation of the plant model in the continuous domain shows that both step and – the more important for the BEAU's application – ramp inputs are easily tracked by the proportional-differential controller. The ramp input is of more interest than the step response because the  $\theta_{err}$  that results from the difference of  $\theta_{pedal} - \theta_{motor}$  is  $\theta_{flexure}$  or the angle of deflection of the flexure. Deflection of the flexure will provide a torque disturbance to the system. As the controller adjusts  $\theta_{motor}$  such that  $\theta_{err} = 0$  the torque of the motor plus the torque disturbance will cause what would usually be a step input to the system to behave like a ramp input.

---

<sup>5</sup>PWM stands for "pulse width modulation" and is a common way to move between digital signals (0 and 1) to analog control voltages.

<sup>6</sup>This change is simply a normalized constant multiplier, so there will be no real effect on the response of the system.

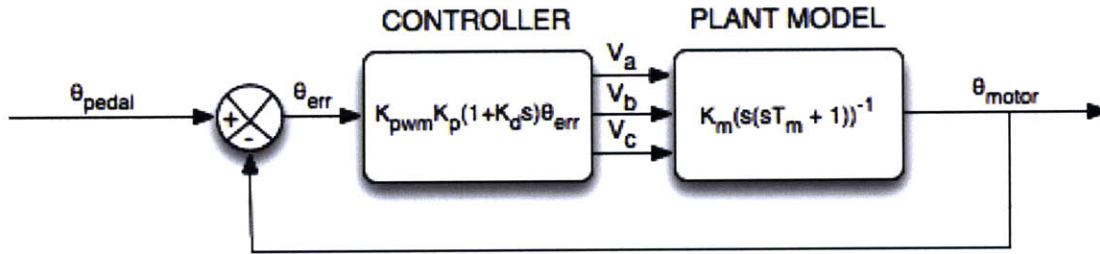


Figure 4.5: This closed loop control loop shows the PD controller, plant, and feedback pathway. The plant model in this control loop is simplified by negating small terms.

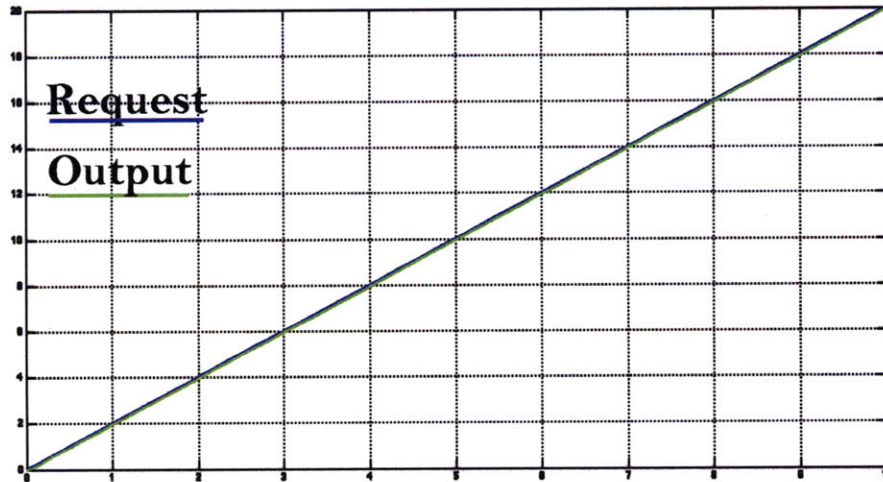


Figure 4.6: Closed loop PD control of the response to a ramp input. Axes are time in seconds for x and degrees for y.

In order to implement this on the Atmel microcontroller used to process the control loop, the PD controller must be transformed into the z-domain. This will allow for discrete time control which can be directly implemented in digital control logic with a known, well controlled sampling period  $T$ .

---

### 4.3. CONTROL HARDWARE

The circuitry for the BEAU is entirely custom designed. This is necessary due to the lack of small, high power motor controllers in a form factor that will work with the BEAU's internal architecture and because the feature-set required by the BEAU is specific enough that a custom board that implements all of the features is more efficient than several, more dedicated boards.

The control hardware for the BEAU is located in one of the three stator structural supports. These supports rigidly connect the BEAU's shaft to the motor stator. This placement allows heat transfer

through the support frame of the BEAU to the outside world through the shaft while also providing an ideal control circuit placement. The batteries and motor are located directly adjacent to the control circuit.

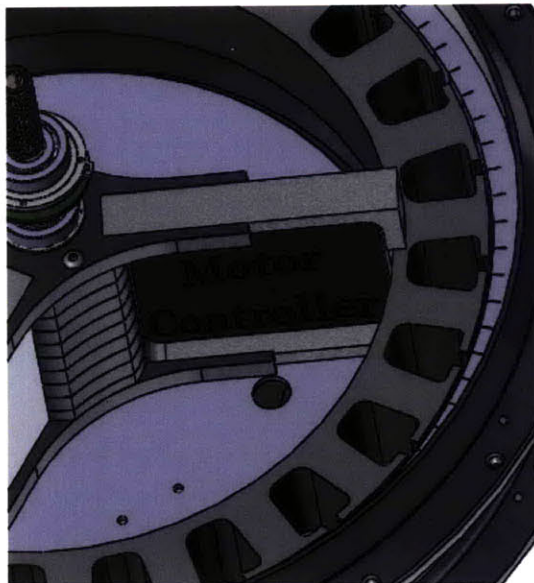


Figure 4.7: The control hardware for the BEAU is located in one of the three supports for the motor armature.

#### 4.3.1. CONTROLLER INPUTS AND OUTPUTS

Physically, the motor control hardware takes  $\theta_{pedal}$ ,  $\theta_{motor}$ ,  $V_a$ ,  $V_b$ ,  $V_c$ , and  $E_{batt}$  as inputs and gives  $PWM_a$ ,  $PWM_b$ , and  $PWM_c$  as outputs from the onboard power MOSFETs. The controller also internally measures  $i_{total}$  with a high power, low resistance current sense resistor.

The controller uses  $\theta_{motor}$ ,  $V_a$ ,  $V_b$ , and  $V_c$  in order to predict the phase angle of the motor  $\alpha$ . This information is used by the internal timing circuitry to produce the properly timed PWM waveforms to drive the motor. PWM is the most commonly used method to control the voltage which the motor receives.

#### PWM

The MOSFETs which drive the motor can only be on or off. This means that at any given time they will provide either 0V or  $V_{batt}$ . Rapid variation between the two states produces a waveform that has a certain percentage on and a certain percentage off. This can be referred to as the duty cycle of the PWM waveform. The motor's electrical characteristics (RL) act as a low pass filter, effectively smoothing the PWM waveform into a more analog voltage. A 20% duty cycle with 10 volts will appear as 2 volts on average[16].



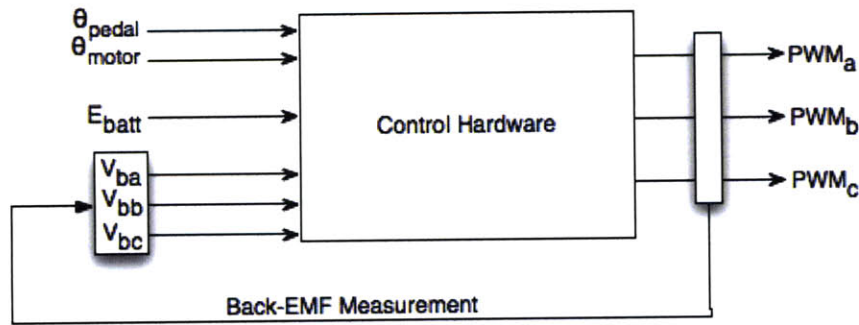


Figure 4.8: The physical inputs and outputs of the controller can be seen in this diagram. Notice that while the back-EMF measurements are external, they technically feed immediately back into the controller.

The energy required between on and off states and the power dissipated by the FET contributes to the *switching power loss*. This loss is dependent on the switching frequency of the PWM signal as well as the rise and fall times for the FET. Care must be taken to minimize the switching power loss[2]. A lower PWM switching frequency means lower average switching power loss, too low will cause the motor to resonate at the PWM frequency, decreasing the efficiency of the motor[19].

#### SENSORS

$\theta_{pedal}$  and  $\theta_{motor}$  are determined through quadrature encoder readings.  $\theta_{motor}$  is read by an ASM magneto-resistive encoder.  $\theta_{pedal}$  is read with a reflective optical encoder by US Digital. The sensors are located on opposite sides of the BEAU, with the pedal encoder actually being located inside the freewheel. The magnetic encoder was chosen over a standard transmissive or reflective encoder because it allows necessary blind-mate assembly.

The sensors in Figure 4.10 provide feedback in terms of  $\theta$ . In order to get  $\frac{d\theta}{dt}$  the microprocessor must take the derivative. The printed circuit board for the pedal encoder read-head and counter IC is located inside the freewheel. It is mounted rigidly to the BEAU's shaft

The encoder board talks to the motor control board over the SPI (serial peripheral interphase) bus. The SPI bus allows the microprocessor to talk to many devices over the same bus. Both encoders are SPI enabled. The microprocessor is in 'master' mode, and enables each device via a chip select I/O pin in order to communicate.

#### MOTOR DRIVE TECHNIQUES

The motor in the BEAU is driven using six MOSFETs. They are connected to each phase in pairs, allowing each gate to cause its respective phase to be directly connected to  $V_{batt}$  or ground (PWM 0 or 1). This is the most common method of three-phase control, and is commonly referred to as a three half H-bridge setup[19].

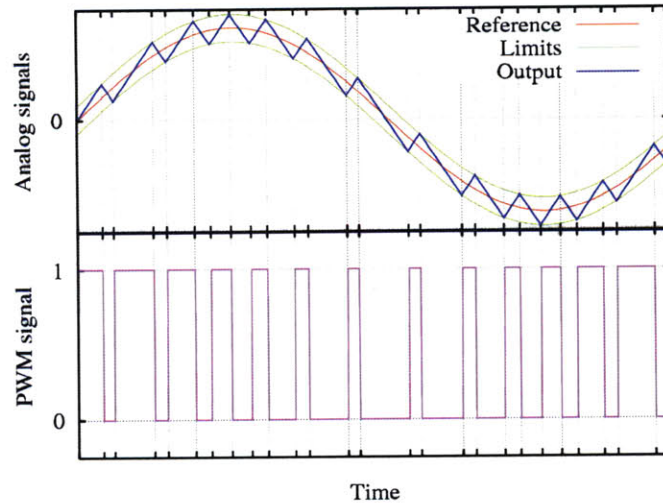


Figure 4.9: A comparison between an analog signal and the corresponding PWM signal. Image by Cyril Buttay.

The half H-Bridge drive allows for very good control of a three-phase brushless motor. Care must be taken to prevent shoot-through, a situation where both high-side and low-side FETs are on at the same time. In this situation the battery is effectively short circuited, or  $V_{batt}$  is connected directly to ground. In order to prevent this most MOSFET drivers have built-in dead times between states and safety latches that prevent both FETs from being on at the same time[20]. The dead time allows the first FET to become fully on or fully off before the next event. The FET turn-on and turn-off times are important factors in motor controller design, as they dictate the frequency at which you can safely provide signals to your motor.

Three-phase motors can either be driven with sinusoidal commutation or trapezoidal commutation. We have seen the math necessary to arrive at the correct sinusoids for sinusoidal commutation in the definition of the closed-loop controller. Trapezoidal commutation creates a step-function that resembles sinusoidal commutation. The motor's electrical dynamics tend to smooth out this type of commutation such that the end result is much like a sine input.

The advantage to the type of six-step commutation shown in Table 4.1 is the ability to turn the MOSFET on for longer periods of time, and therefore eliminate many frequency dependent issues. Keep in mind that the electrical angle is equal to sixteen times the mechanical angle. Even at this increased rate trapezoidal commutation decreases power loss in the FETs by allowing them to switch *much* slower than they would with sinusoidal drive[13].

The major drawback to trapezoidal control is the fact that it requires larger passive components on the motor controller, and does not result in as smooth a torque versus electrical angle curve. In general the mechanical and electrical inertia and impedance generating features will hide this torque discontinuity fairly well, but in situations where very precise torque output is required,

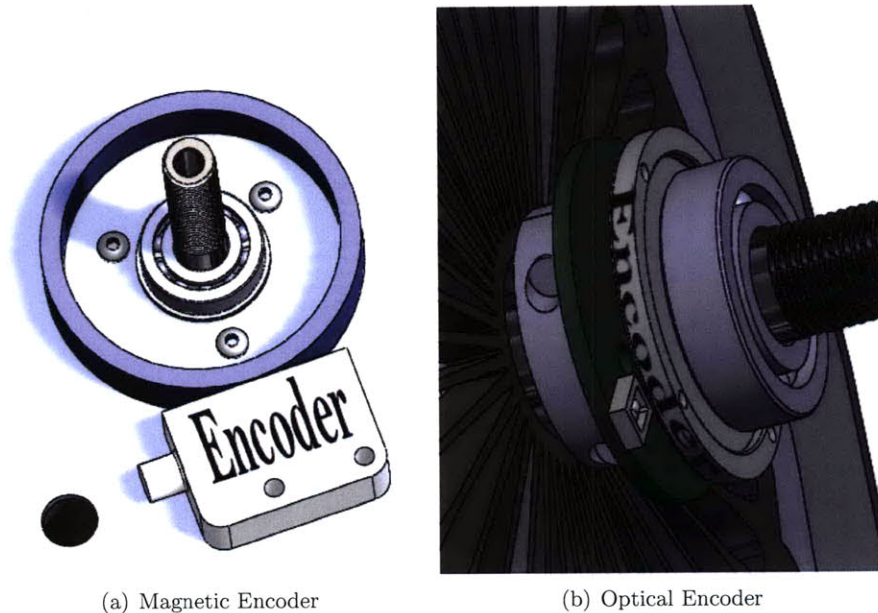


Figure 4.10: Locations of the two encoders in the BEAU. These are the only two sensors used by the BEAU.

trapezoidal control will not work<sup>7</sup>.

In the case of the BEAU trapezoidal control will work wonderfully. The large mass of the bicycle and rider combined with the – small but non-negligible – rotational inertia of the wheel and motor casing will effectively eliminate any torque ripples in terms of user experience. Also, these torque ripples occur once every state change, which means that a ripple happens six times every 360 electrical degrees, which happens 16 times every 360 mechanical degrees. Six times 16 is a big number, or 96. This frequency of ripples is fast enough to easily be smoothed out by inertial factors[8].

#### 4.3.2. THE CONTROL BOARD AND COMPONENTS

The main controller uses an Atmel ATMEGA165PA microprocessor for all digital processing. The 165PA sends signals to the Allegro Microsystems A4935 automotive 3-phase MOSFET driver which takes care of the gate drive dynamics. The MOSFETs are Fairchild Semiconductor’s FDB024N06 120A, 60V N-Channel, metal-oxide discrete semiconductor product.

The majority of the motor control circuit is made up of passives. Passives are components like resistors, capacitors, diodes, and inductors. The passives provide biasing internal IC settings, protection from high currents, and filtering from noisy signals, among other things, such as decoupling, voltage shifting, and timing.

<sup>7</sup>On that note, neither will sinusoidal control without proper dead-time PWM waveform corrections that are somewhat non-trivial to perform but can be easily implemented via a state machine on a microprocessor.



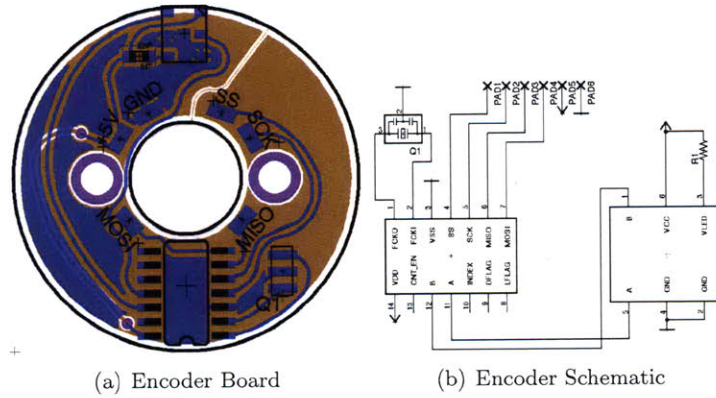


Figure 4.11: The board layout and schematic diagram for the pedal encoder.

Table 4.1: The six-step method for motor commutation.

Electrical Angle (radians)	$A_{HIGH}$	$B_{HIGH}$	$C_{HIGH}$	$A_{LOW}$	$B_{LOW}$	$C_{LOW}$
$0 \rightarrow \frac{\pi}{3}$	1	0	0	0	1	1
$\frac{\pi}{3} \rightarrow \frac{2\pi}{3}$	1	1	0	0	0	1
$\frac{2\pi}{3} \rightarrow \pi$	0	1	0	1	0	1
$\pi \rightarrow \frac{4\pi}{3}$	0	1	1	1	0	0
$\frac{4\pi}{3} \rightarrow \frac{5\pi}{3}$	0	0	1	1	1	0
$\frac{5\pi}{3} \rightarrow 2\pi$	1	0	1	0	1	0

A well designed controller for the BEAU must accomplish the following:

1. Not blow up. As funny as this sounds, it is quite common for motor controllers. In fact the chances of a designer succeeding on the first attempt to design and build a new controller from scratch is very low and usually the failure mode is a component dramatically failing in the form of a fireball. This stresses how important it is to protect the delicate ICs on the controller from high voltage and current spikes.
2. Be heat tolerant. The BEAU does not have a good way to remove heat from inside its casing. The motor, batteries, and controller will all generate a large amount of heat. At normal motoring speeds the motor will be running at 200 - 300 watts. With a mere 5% inefficiency, 10 - 15 watts will be dissipated inside the casing. Unfortunately the inefficiencies are closer to 15% - 20%.
3. Reliably control the motor. Motor control timing is not easy<sup>TM</sup>. The hardware must be able to reliably discern from the back-EMF and encoder inputs exactly where in its electrical phase the motor is located at all times. A fault with this measurement will result in unwanted bucking of the motor[16].

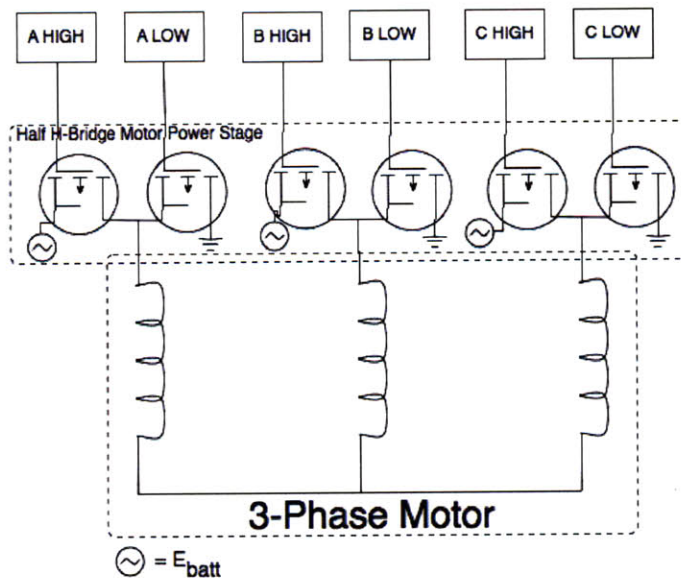


Figure 4.12: The six inputs that drive a three-phase motor and the structure of the half H-bridge.

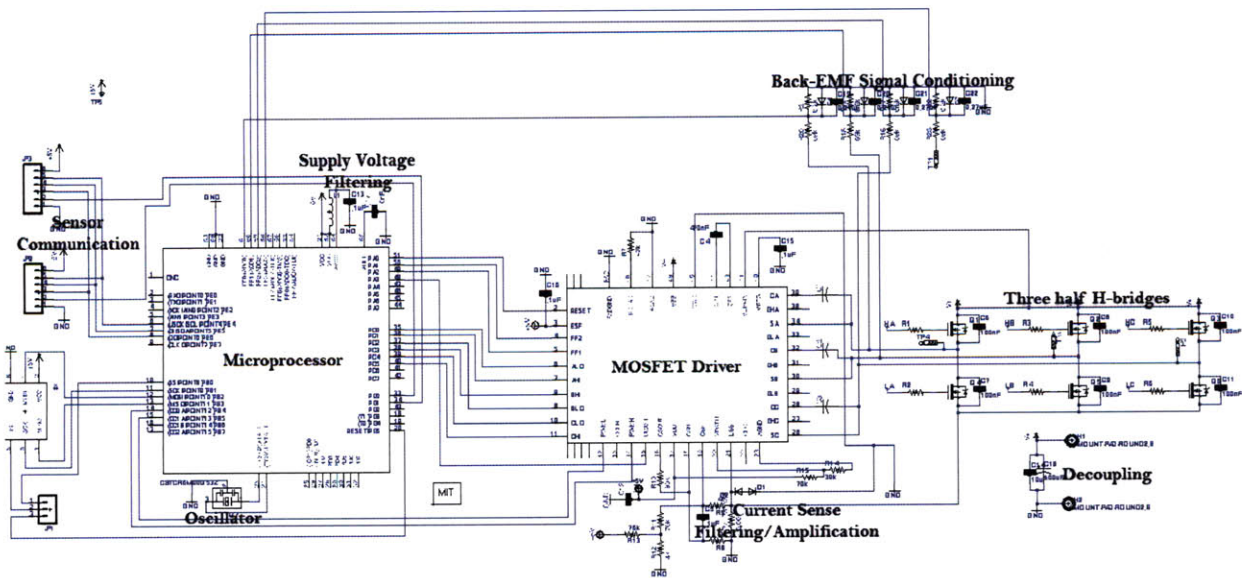


Figure 4.13: The motor controller schematic is labeled with items of interest.

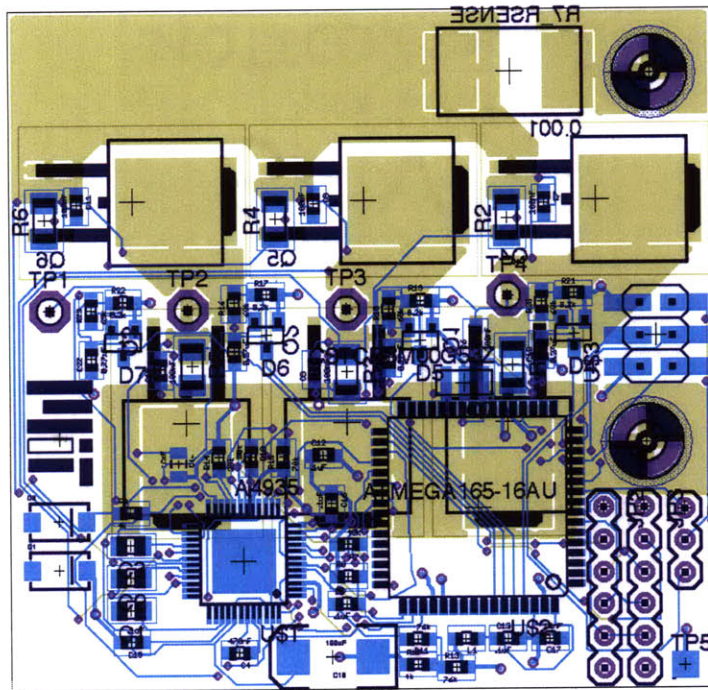


Figure 4.14: The motor controller board layout. This is a four layer board with internal ground and logic supply planes that are not shown for clarity.



---

## 5.0. THE TORQUE SENSOR: A COMPLETELY INTERNAL METHOD OF MEASURING USER TORQUE

---

### 5.1. INTRODUCTION TO FLEXURES

A flexure is a device consisting of two or more rigid bodies attached via compliant elements in order to allow for well-defined, repeatable motion. Flexures can be monolithic (a single piece of material) or they can consist of several separate parts that are attached together[17]. Because flexures almost exclusively operate in the elastic regime, they can be thought of as specialized springs that allow atomic accuracy at low actuation force. While they are heavily used in high-precision devices such as microscopes, mass balances, optics, and clocks, flexures are also found in many common consumer products such as computers, boom-boxes, and even MP3 players[17].

The origins of the flexure date back to the discovery of classic materials mechanics theory, with notable contributions by Galileo, Hooke, Marriott, and Harrison[17]. With the understanding of linear elasticity came the ability to build new devices that would have otherwise been left to chance. The standardization of material properties measurement combined with the simplicity of linear elastic mechanics allowed theoretical predictions in flexure design to be realized. While the use of the flexure is not new – dating back to the 1600's – the newly available precision fabrication technology such as 5-axis CNC machining, CNC wire electromagnetic discharge machining, and 3D printing technologies such as selective laser sintering (SLS) and stereolithographic (SL) machining have allowed flexure designs that were previously too costly or impossible to create to become common.

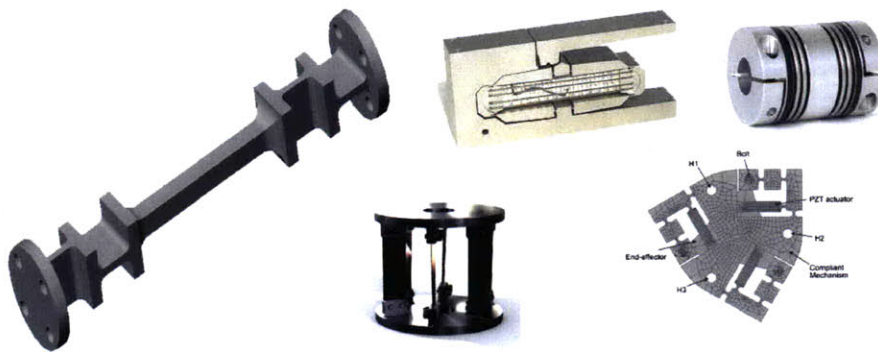


Figure 5.1: Various types of flexures that are commonly used.



### 5.1.1. ADVANTAGES OF FLEXURES

1. Flexures do not “wear out.” Because the concepts of fatigue and yielding are well understood, a flexure can be designed to provide the exact level of performance throughout its life. Moreover, flexures do not have sliding parts, bearings, or fluids.
2. Flexures have advantageous manufacturing qualities. Generally a flexure can be produced inexpensively and easily. Assembly is either non-existent or very simple, especially given that many flexures are made from a single piece of material[3].
3. In a controlled system flexures offer extremely accurate and smooth displacements. Even complex flexure mechanisms allow displacements to be linear and predictable down to atomic resolutions. Manufacturing tolerance errors generally result in a flexure following a non-ideal path, but it will do so linearly while maintaining a linear relationship between applied force and displacement. More on this later[3].
4. Because flexures can be made from a single piece of material, stress concentrations due to manufacturing processes such as welding, clamping, and glueing can be avoided, preventing unwanted residual stresses that can lead to non-linearities, manufacturing defects, and untimely failure[17].
5. It is possible to design mechanisms that provide controlled, predictable leveraging as well as mechanisms that are insensitive to changes in environment, such as temperature.

### 5.1.2. DISADVANTAGES OF FLEXURES

1. It is very difficult to predict the exact force/displacement curve of a new design. Variations in material (stock source, inhomogeneities, etc.) and inevitable out-of-nanometer-tolerance issues prevent a direct link between design and theory and the physical behavior of the flexure. In practice this is overcome through calibration countermeasures.
2. Flexures are utterly restricted to small displacements compared to multi-body mechanisms of similar size. This stems from the requirement that the material of which the flexure is made must remain within its allowable fatigue adjusted linear elastic regime[17].
3. Out of plane stiffness (the plane that is not intended to displace) is low in comparison to other mechanisms, and in plane stiffness is higher in comparison to commensurable counterparts, such as those that employ bearings. Generally flexures are coupled with external structures that both prevent over and out of plane actuation.
4. Flexures do not perform well under large loads. This loading can be a direct or indirect loading. Indirect loading is especially disadvantageous because it can cause early fatigue and failure of a flexure’s spring elements as well as decrease the overall stiffness of the system even through only inertial effects[17].
5. Accidental loading can overload the flexure material causing fatigue, work hardening and catastrophic failure. A single loading scenario that takes the device into the plastic regime will permanently change its characteristics even if it continues to perform linearly.

With the BEAU in mind, the goals of the flexure that serves as the rider torque sensor are twofold<sup>1</sup>: At a given displacement provide a specific, known force and provide a specific, known displacement at a given force. While these may seem conversely related, there are different design approaches to each depending on which result is most important. In the case of the BEAU, it is most important to have a known displacement at a given force.

The following flexure design description will not address all of the disadvantages presented. This is because calibration, plane stiffness, and accidental loading lie in the realm of the BEAU's control system and mechanical design. While flexures do have real and nontrivial concerns, the design decisions required to plan for these concerns do not outweigh the benefits of a flexure for use as a torque sensor in the BEAU.

---

## 5.2. THE RADIAL FLEXURE DESIGN AND THEORY

Like most types of design, the process of designing a flexure begins with the determination of functional requirements for the device. For flexure design the functional requirements will fall into the realm of required displacements, size constraints, temperature tolerance, force to displacement relationships, and displacement multiplication requirements. The radial flexure used in the BEAU is fairly simple. In fact, its design is as simple as possible while achieving the displacement and force tolerance required.

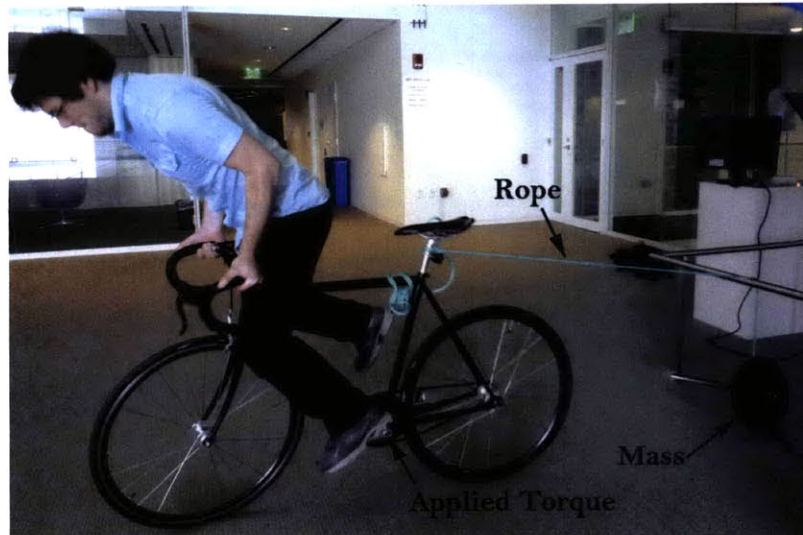


Figure 5.2: The experimental setup for determining the maximum torque a rider can apply to a bicycle wheel.

The BEAU's flexure must be capable of displacement through the range of torque applied to it. On a standard bicycle, the torque is supplied to the pedals and through the chain. In order to determine the torque that the flexure will see, a bicycle was attached to a rope at the seat location.

---

<sup>1</sup>These are also generally the goals of all flexure designs

The rope ran horizontally behind the bike to a pulley which changed the rope direction to vertical. Weights were attached to the vertical section of the rope. A representative average rider was placed on the bike and asked to attempt to lift the weights from the ground by riding the bicycle. The weight on the rope was increased in 11N (2.5 pound) increments until it was no longer possible to lift the weight. The weight that no rider was able to lift was 155N. Because the torque on the flexure and the pull on the rope can be directly related by the radius of the real wheel, we can see that  $\tau = F * r$ . If the wheel radius is 0.337m, the force acting on the flexure at maximum torque is 52.4Nm. In further calculations this torque is rounded to 50Nm.

### 5.2.1. PHYSICAL ENVELOPE DEFINITION

Before we can begin to determine how the flexure will look the space envelope and deflection requirements must also be known. These values are harder to calculate because they rely on other aspects of the BEAU's design. The flexure is located in the freewheel side of the wheel hub (the right side from the point of view of a rider seated on the bicycle). With the given structural requirements and space requirements of the hub the maximum allowable thickness of the flexure in the axial direction is 5.0mm. The maximum radius of the flexure has more freedom, but without sacrificing aesthetic symmetry between the left and right sides of the wheel hub the flexure must have a radius equal to or less than 40mm. The deflection of the flexure is dependent on the sensor used to measure the deflection. The BEAU uses an incremental reflective optical encoder from US Digital that provides a quadrature resolution of 8 counts per degree. In order to have enough data to generate a smooth control curve, at least 30 counts are necessary. Five degrees of deflection gives 40 counts. The flexure is designed with a deflection goal of 5 degrees.

Other requirements of the flexure include the necessity of space for the central shaft plus clearance as well as space for a central mounting coupling between the flexure and the freewheel. Based on the coupling's torque requirements the inner 'hole' in the flexure was determined to be roughly 16mm (a 16mm x 1 threaded hole).

### 5.2.2. BASIC BEAM THEORY

With this in mind we can begin to realize how the flexure might look in its simplest form. Assuming a maximum spring element length of 26mm the simplest element shape is a beam with a constant rectangular cross-section over its length. In reality each spring element in the flexure deflects radially in nature but fortunately a deflection of five degrees allows us to assume cartesian deflection without sacrificing accuracy. This assumption also allows us to look at one spring element as a simple beam deflection problem[11].

The simplest beam case would be that of a simply supported cantilever with a point force ( $P$ ) applied at the free end. In this case we can see that the shear on the beam would be  $P$  for all  $x$  where  $x$  equals zero to the length of the beam ( $l$ ). The moment on the beam is simply the internal torque the beam feels at any point  $x$ . In this case it would be equal to  $P * (l - x)$ , showing that the moment is highest at the base of the beam [15]. This makes sense from our intuition about torque at an applied distance. Given our expressions for shear and moment, we can integrate to find the angle of the beam under load as a function of  $x$ :



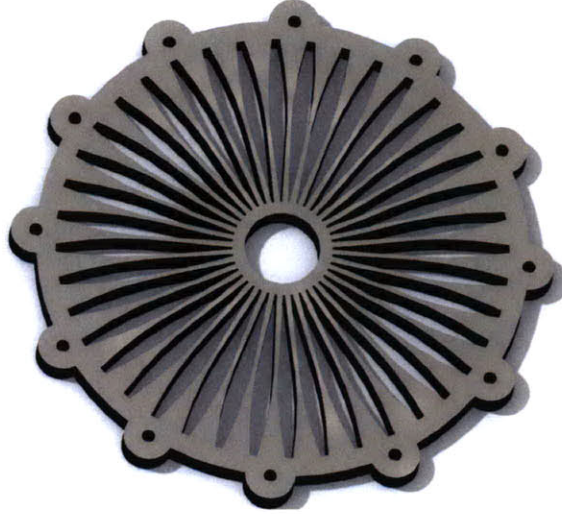


Figure 5.3: A 3D representation of the flexure used in the BEAU as a torque sensor.

$$\begin{aligned}
 \theta(x) &= \int_{x=0}^l \frac{M(x)}{EI} dx + C \\
 \theta(x) &= \frac{Px}{2EI}(x-l) + Cx
 \end{aligned} \tag{5.1}$$

Where  $E$  is the material's Young's Modulus and  $I$  is the material's area moment of inertia. Integrating again gives us the expression for the deflection of the beam at any point  $x$ . Both constants of integration are zero and  $x$  is replaced with  $l$  to show the deflection of the beam's tip as a function of the applied force  $P$ .

$$\begin{aligned}
 \delta(x) &= \int_{x=0}^l \frac{Px}{2EI}(l-x) + Cx \\
 \delta(x) &= \frac{Px^2}{6EI}(3l-x) \Big|_{x=l} \\
 \delta(P) &= \frac{Pl^3}{3EI}
 \end{aligned} \tag{5.2}$$

Using this equation we can determine the deflection associated with a given applied force; this assumes knowledge of the beam's physical characteristics. Currently the only physical characteristics that are unknown are the thickness of the beam in the direction of force ( $t$ ) and the Young's Modulus of the material. Before making the required rearrangements to create an expression for  $t$  as a function of known values (we can insert values of  $E$  based on the material choices at hand) it is important to check the validity of this theory to the real object we are attempting to describe[9].

A simple flexure was designed in SolidWorks, a 3D CAD program, to use in the validation of the theoretical flexure model. The 3D flexure model was subjected to FEA testing to create a force versus deflection graph. Comparing the FEA data to equation (5.2), we can see that the theoretical data and the FEA data appear to differ from each other by a factor of four.

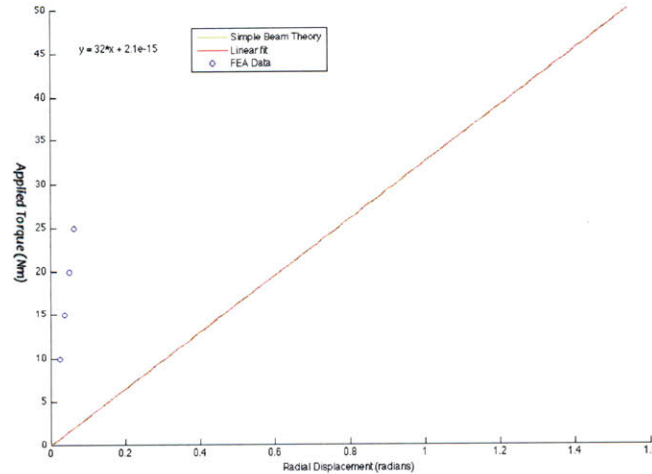


Figure 5.4: The simple cantilever beam force deflection graph vs FEA data.

With the simple beam deflection model the beam's tip is allowed to freely rotate with the deflection of the beam, but in the case of the flexure it is constrained to remain parallel to the flexure's outer surface, or tangential to the flexure's inner and outer rings. This can be modeled as a restoring moment applied to the tip of the beam, but because the moment is a function of angle which is a function of torque, the solution is more interesting than a simple textbook equation[15].

### 5.2.3. CARTESIAN BEAM BENDING DUE TO ROTATION

The radial flexure technically operates in the polar regime. Because the spring elements are relatively constant in thickness and do not vary proportionally to  $r$  or  $\theta$  in any way, solving the system in polar coordinates will only make the solution more complex with little to no added accuracy. Figure 5.5 shows the way the flexure's spring elements will be modeled in order to recover the most accurate prediction of its deflection response. In comparison to the deflection of a simple cantilever beam with  $\theta(x = 0) = 0$  (That is, the base of the beam is constrained to be perpendicular to an imaginary mounting wall that is immovable.), the  $\theta(x = l)$  solution produces a negative result because the beam is actually forced to rotate past horizontal in the opposite direction that it would usually rotate under unconstrained loading.

For those unfamiliar with mechanics, the first beam's (a constant cross-section cantilever with one end fixed) deflected shape looks similar to a diving board with a diver standing at its tip.<sup>2</sup> The tip of the diving board is oriented vertically when no diver is present. During deflection the tip angle

<sup>2</sup>Although it may seem that the deflection of a diving board and this type of beam are the same, they are not.

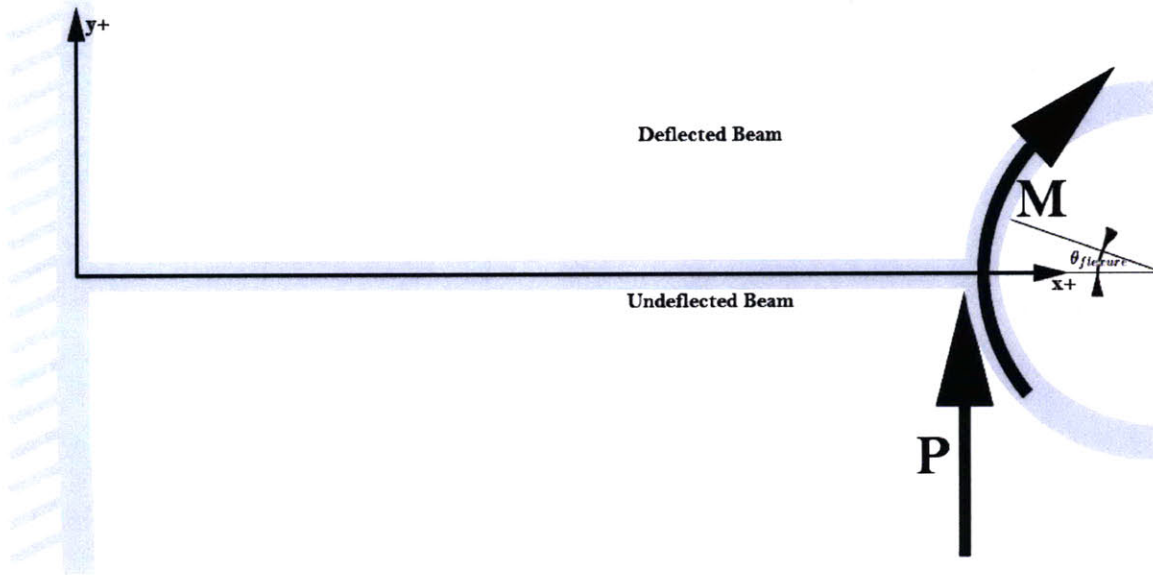


Figure 5.5: The simple cantilever beam model with a restoring moment that maintains the beam end  $\theta(x)|_{x=l} \parallel \theta_{flexure}$ . Pay close attention to the signs of each value.

decreases because of the rotation of the board. Now imagine that instead of a diver we attached a large wheel to the tip of the board such that the tip angle must remain tangent with the circle – in other words we rigidly attach it to the wheel. If we put a torque on the wheel that produces a force at the diving board equal to that of the diver, we will see that the deflection shape has changed noticeably. If we assume that the board is attached to the wheel at a point that is horizontal and collinear with the wheel's center, we can see that as the wheel rotates in order to produce deflection in the board, the point of attachment with the wheel moves down. The tangent angle associated with this point for this type of rotation is a positive change in angle.

An easy way to physically visualize this can be to orient your pointer finger with the palm of your hand facing in the direction of deflection. Point at the center of a cylindrical object such that the line of your fingers is parallel to the axis of most efficient rolling for the cylinder. Touch the point that is being pointed at and imagine that that is the tangent condition. Bending your finger simulates deflection, notice the angle change of the tip of your finger. Now look at the cylinder and notice the angle the tip of your finger would have to have in order to deflect and remain rigidly attached to the cylinder.

To begin, we can recall from the well known Myosotis Sylvatica reference in materials mechanics most easily located in section 8.17 of [21]. In order to find the  $\delta(P)$  for the beam – the stiffness constant – the general equations for  $\theta$  and  $\delta$  are used. The moment and transverse shear equations

---

A diving board actually deflects up between the base point and the pivot point, causing the moment experienced at the base of the board to be opposite in sign to that in this simple case.

are also presented for completeness.

$$\begin{aligned} V &= R_A - W(x - a)^0 \\ M &= M_A + R_A x - W(x - a) \\ \theta &= \theta_A + \frac{M_A x}{EI} + \frac{R_A x^2}{2EI} - \frac{W}{2EI}(x - a)^2 \end{aligned} \quad (5.3)$$

$$\delta = \delta_A + \theta_A x + \frac{M_A x^2}{2EI} + \frac{R_A x^3}{6EI} - \frac{W}{6EI}(x - a)^3 \quad (5.4)$$

From the free-body diagram of the beam and Equations (5.3) and (5.4), we can arrive at a specific description of  $\theta$  and  $\delta$  in terms of the moment and the shear force applied to the beam. Unfortunately, while the shear force is known, the moment is not. This means that we need a way to determine the value of the moment. To begin:

$$\theta = \frac{Ml}{EI} + \frac{Pl^2}{2EI} \quad (5.5)$$

$$\delta = \frac{Ml^2}{2EI} + \frac{Pl^2}{6EI} \quad (5.6)$$

With eight-thousandths of a percent error over the range of operation for the BEAU's flexure, we can make the assumption that  $\delta = r\theta$ , which allows Equations (5.5) and (5.6) to be set equal to each other, namely  $\frac{Mlr}{EI} + \frac{Pl^2 r}{2EI} = \frac{Ml^2}{2EI} + \frac{Pl^3}{6EI}$ . Solving shows that  $M = P\left[\frac{6r-3l}{2l^2-3rl}\right]$ . We also know that  $\tau = n(M + Pr)$  where  $n$  is the number of spring elements in the flexure[9]. The torque is not equal to simply  $Pr$  because both the moment and the linear force are contributions of the torque to the beam and are not results of one another as is the case in simpler beam deflection solutions. Substituting our value for  $P$  into the torque equation we can see that

$$\tau = nP \left[ \frac{2l^2 - 6rl + 6r^2}{6r - 3l} \right] \quad (5.7)$$

and from Equation (5.6) we can see that

$$\delta = \frac{Pl^3}{6EI} \left( \frac{l - r}{2r - l} \right) \quad (5.8)$$

Combining Equations (5.7) and (5.8) yields

$$\delta = \tau \frac{l^3}{6nEI} \left[ \frac{l - r}{2r - l} \right] \left[ \frac{6r - 3l}{2l^2 - 6rl + 6r^2} \right]. \quad (5.9)$$

If we compare the results of Equation (5.9) with FEA by plotting, we can see that to within a reasonable error tolerance this representation of the  $\delta(\tau)$  is sufficient to design a flexure without the use of FEA until the design verification steps.



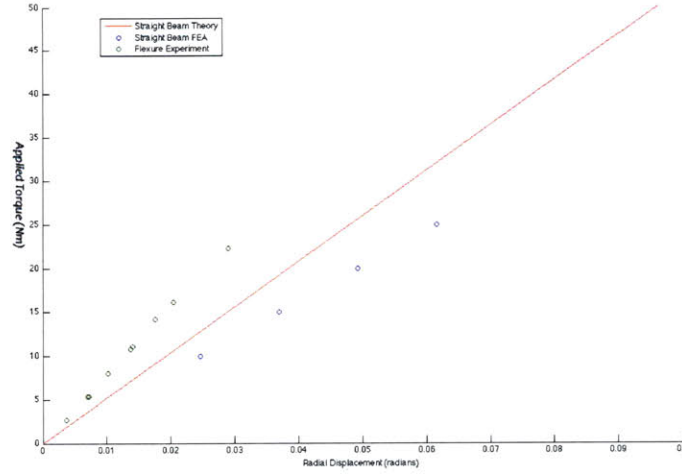


Figure 5.6: The data from theory and FEA for the beam bending model that takes into account the tip rotation condition caused by the rotation of the inner hub.

#### 5.2.4. THE EFFECTS OF SHEAR AND STRAIN

Before moving forward with the analysis it is important to investigate the effects of forces that are not yet accounted for in this model; namely shear and strain. Strain is especially interesting because the radial nature of the flexure keeps the beams from changing length during deflection which is generally not the case in most flexure designs. Using energy methods we can arrive at an expression for the total deflection of the beam that takes shear, moment, and strain effects into account:

$$\frac{1}{2}P\delta = \int_{x=0}^l \frac{f_s V^2 dx}{2GA} + \int_{x=0}^l \frac{f_s M^2 dx}{2EI} + \int_{x=0}^l \frac{f_s N^2 dx}{2AE} \quad (5.10)$$

Solving for shear and moment are relatively easy. Unfortunately the strain on the beam is very difficult to solve because the axial force on the beam is dependent on its change of length under deflection. Since we know that  $\epsilon = \frac{l(P)}{l_0}$  and  $N = \epsilon EA$  we can find N if the length of the deflected beam is known.

$$s = \int_a^b \left[1 + \frac{dy^2}{dx}\right]^{\frac{1}{2}} dx \quad (5.11)$$

Applying the characteristics of the flexure beam and simplifying to dimensionless parameters, we can see that

$$\frac{l(P)}{l_0} = \int_0^1 [1 + (c(\alpha^2 - \alpha))^2]^{\frac{1}{2}} d\alpha \quad (5.12)$$

where  $c = \frac{Pl^2}{2EI}$ . This integral is unsolvable. A closed form solution for strain cannot be found.

Using numerical analysis we can provide a value for strain as a function of P for the following deflection equation that results from equation (5.10).<sup>3</sup>

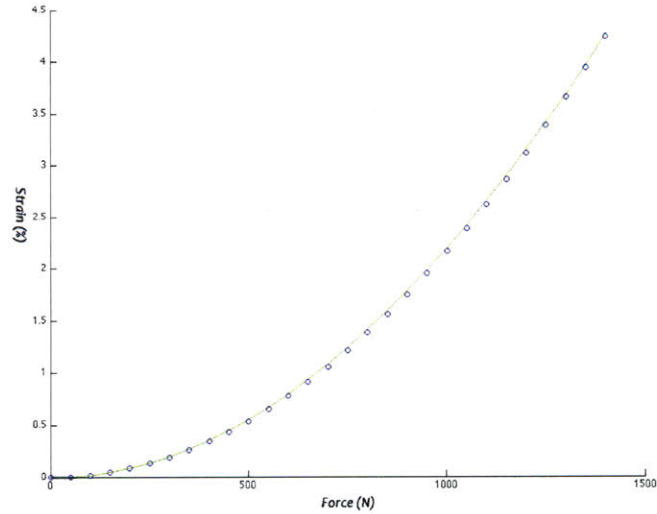


Figure 5.7: A numerical solution for the integral in equation (5.12). The range of importance for the BEAU’s flexure can be approximated by the form  $\frac{(PC_1)^2}{C_2}$  to a high degree of accuracy, as can be seen in the figure.

$$\delta = \frac{3Pl(1 + \nu)}{5Ewt} + \frac{Pl^3}{Ewt^3} + \frac{E\epsilon^2wtl}{2P} \quad (5.13)$$

The graphs below represent the force versus deflection curves for the model. The first takes into account shear and strain, the second does not. Because the shear and strain contributions are so small at this deflection it is not necessary to consider them in the design of the flexure elements.

In reality it is highly advantageous that shear and strain do not come into play with this type of flexure design. A simple relationship between applied force and displacement means that we can arrive at a general idea (number of spring elements, rough thickness, material, etc.) of the flexure quickly and accurately, making the time spent modeling in CAD and running FEA smaller and less tedious. Without this analysis *all* of the design decisions would have to be made through trial and error of educated guesses that are validated via FEA.<sup>4</sup>

<sup>3</sup>You may notice that the equation for the moment contribution in this equation does not look consistent with  $M = P[\frac{6r-3l}{2l^2-3rl}]$ . It isn’t. The results here are computed with a perpendicular condition which simplifies the math while maintaining accuracy.

<sup>4</sup>In practice this takes a very long time. Because of the number of variables involved in the process (number of spring elements, thickness profile, depth profile, inner diameter, outer diameter, material) it is possible to save a designer weeks of design time using the theoretical analysis presented in this section.

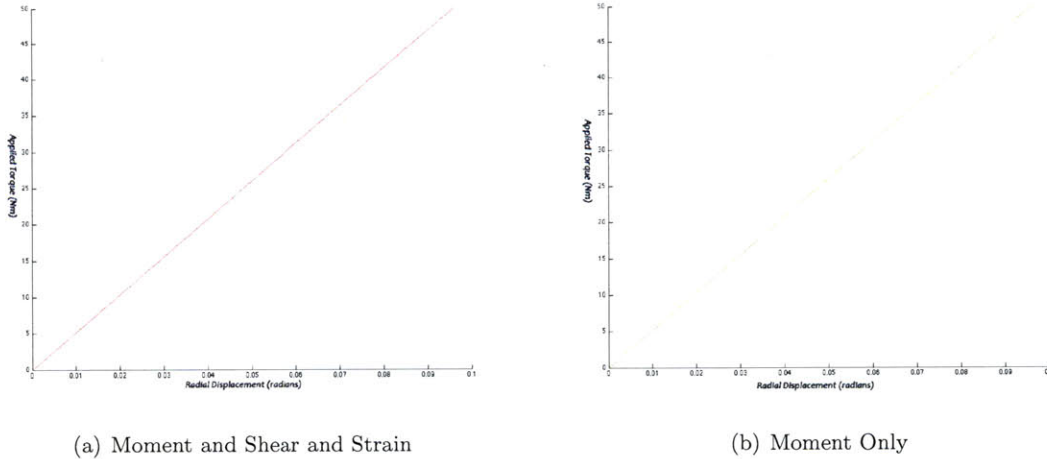


Figure 5.8: A comparison of the theoretical torque versus displacement of a flexure taking into account moment, shear, and strain, and only moment. Because the shear and strain effects are negligible and can be ignored as evidenced in the figures above.

### 5.2.5. FULLY-STRESSED BEAMS

At this point the deflection for a given force is well classified in the elastic regime. In order to determine if a given design which satisfies a the required set of force/deflection parameters lies within the elastic regime we must look at the stress on the spring element of the flexure. We can see that

$$\sigma = \frac{6P(\frac{1}{2}l - x)}{wt^2} \tag{5.14}$$

for the beam under consideration. A plot of stress versus  $x$  for  $x = 0$  to  $l$  shows the maximum stress on the beam at each point along its length. For reference the maximum stress is located at  $y = \frac{t}{2}$ .

Since the stress is the highest at the ends of the beam it is prudent to consider increasing the thickness of the beam at those locations in order to create a beam with a higher stress tolerance while maintaining as much of its deflection as possible. If we consider the fully stressed beam scenario – the situation where the stress is constant over the entire length of the beam – we can get an idea of how the beam should be designed in order to allow for the most force on the beam[11]. The fully stressed beam outline in Equation (5.10) takes only stress due to bending into account, but the added axial stress component does not significantly alter the curve (other than preventing it from actually hitting zero) because the axial stress component is small for deflections of this magnitude.

Generally flexures are designed using the notch technique. This technique uses a relatively thick beam during most of its length. At the location of movement (deflection), a semicircular notch is taken from both sides of the beam to reduce its thickness to attain the required deflection/force

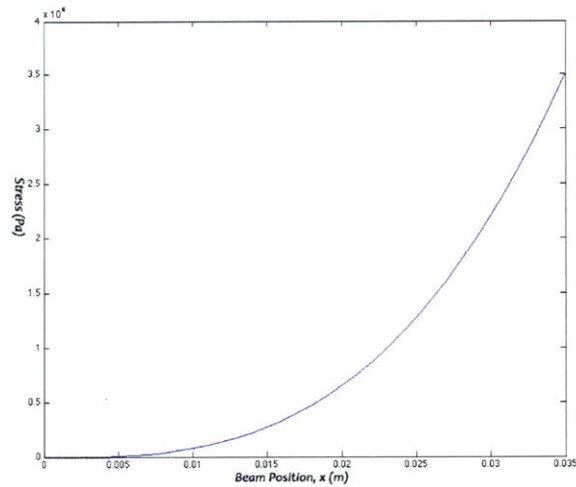


Figure 5.9:  $\sigma(x)$  for a beam with constant cross-section. While FEA is able to give an exact stress concentration for a given design, this simple analysis provides accurate enough results to guide design decisions.

relationship. This technique prevents the rest of the beam from undergoing relevant deflection by keeping it much larger than the notch size. Unfortunately in the design of the flexure for the BEAU, there is not enough space in the radial direction to allow for such a design. Also, this design does not allow for as much deflection since all of the deflection of the beam is concentrated at the notch point. Radial flexures are therefore slightly more difficult to design because they rely on their beams to approach the fully stressed case in order to provide the force/displacement values required without having large stress concentrations at the attachment points.

The most important idea to take away from this fully-stressed beam description is that the spring elements on a radial flexure should be wider at the connection points than in the middle. The shape of the beam should then resemble a lopsided bow-tie<sup>5</sup>. Generally the exact shape of the beam is determined by educated guesses and trial and error in FEA. While this may not initially seem to be the optimal solution, it provides accurate results for complex shapes much faster than can be determined theoretically.

---

### 5.3. THE FABRICATION PROCESS OF THE BEAU'S RADIAL FLEXURE

The flexure for the BEAU was fabricated using wire electric discharge machining (wire EDM) – sometimes referred to as spark machining. The process works by creating a situation in which a tool electrode and workpiece electrode are placed in close proximity such that sparks form between the two. In this process material is removed from both pieces. A non-conductive fluid (usually

---

<sup>5</sup>The lopsided effect is due to the inner circumference of the flexure. There is not enough length over this circumference to provide adequate width to satisfy the fully stressed criteria without decreasing the length of the spring elements



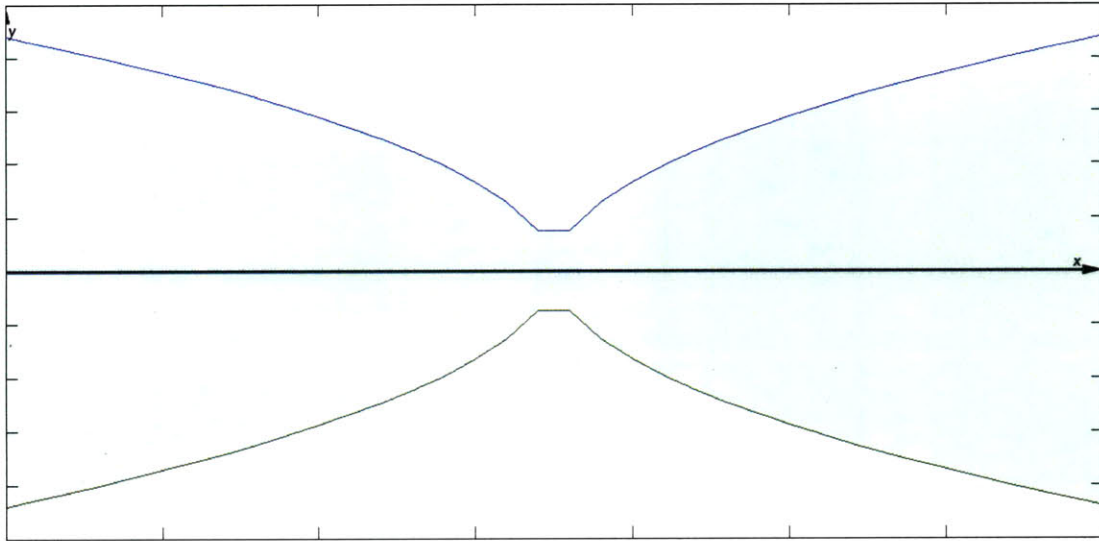


Figure 5.10: A graph of  $y(x)$  of a fully stressed beam. Note that both  $y(x)$  and  $-y(x)$  are plotted to give a representation of  $t(x)$ .

deionized water) flows between the electrodes in order to carry away removed material and prevent shorting. Because both electrodes experience erosion due to the sparking process, the wire used to cut the workpiece must be constantly refreshed. This is accomplished through the use of a spool and continuous feed of wire[3].

Wire EDM can use a very small diameter tool electrode – as small as 0.1mm in diameter. Typical wires are 0.25mm. This creates a cutting path size of roughly  $0.34\text{mm}^6$ . Typical tolerances on wire EDM machines is 0.004mm. The BEAU’s flexure requires wire EDM because of the precision required in the thicknesses of the spring elements and a small kerf diameter offered by small wires which allowed for small feature sizes.

Now that general characteristics such as number of spring elements, spring element thickness, and general spring element shape can be determined mathematically, we need to consider the material from which the flexure will be made. For the BEAU’s flexure the following materials were considered:

The “Ratio” and “ $\epsilon_{max}$ ” columns give insight into which materials are better suited for flexure design. The lower the ratio, the more optimal the material. Conversely the higher the  $\epsilon_{max}$  the better the material (since the two are just the inverse of each other). The BEAU’s flexure requires a very low ratio as well as a very high Young’s modulus to function properly. Because the price difference between the high grades of steel and aluminum that would be suited for the flexure and grade 5 titanium is small, grade 5 titanium was chosen. It offers extreme toughness and high strength.

The BEAU’s flexure has spring elements that are up to 35mm long. In order to deflect 5 degrees

<sup>6</sup>The exact cutting path size, or kerf, can be determined during machine calibration. Typically the value of the kerf is very consistent, but the exact value more difficult to exactly calculate than it is to measure.

Table 5.1: Materials Selection Table for Flexure Design

Materials	E	$\sigma_{yield}$	Ratio ( $\frac{E}{\sigma_{yield}}$ )	$\epsilon_{max}$
5160 Spring Steel	205GPa	275MPa	745	$1.34 * 10^{-3}$
410 Stainless Steel	200GPa	1225MPa	163	$6.13 * 10^{-3}$
6063 T6 Aluminum	68.9GPa	214MPa	322	$3.11 * 10^{-3}$
6061 T6 Aluminum	68.9GPa	276MPa	249	$4.02 * 10^{-3}$
7075 T6 Aluminum	71.7GPa	462MPa	155	$6.45 * 10^{-3}$
Titanium Grade 5	110GPa	828MPa	133	$7.53 * 10^{-3}$

each spring element must be less than a certain thickness  $t$  in order to bend without leaving the elastic regime. Because the relationship between stress and deflection are known,  $t$  can be estimated using

$$t = \frac{\sigma l^2}{3E\delta}. \tag{5.15}$$

Using the parameters that are known, we can see that  $t$  must be slightly less than 1mm or 0.994mm. Given spring elements of this thickness, we can determine the number of spring elements necessary to support a torque on the flexure of 50Nm. We can solve equation (5.14) for  $P$  at  $x = l$ , which will give the force that one spring element can support. From simple physics  $F = \frac{\tau}{r}$ . Combining gives

$$n = \frac{\tau 3l}{r\sigma w t^2}. \tag{5.16}$$

Substituting values gives us an answer of 38.8 spring elements. The flexure in the BEAU uses 40 spring elements. It is clear from these values that the theoretical analysis is able to provide the designer with valuable insight that would otherwise not exist. The ability to calculate approximate spring element thicknesses and numbers for an arbitrary radial flexure before entering the physical design stage can save weeks of design time.

FEA analysis of the BEAU flexure is presented in Figures 5.12 and 5.14. The results allow a reasonable degree of assurance that the design will function as intended in its physical implementation.

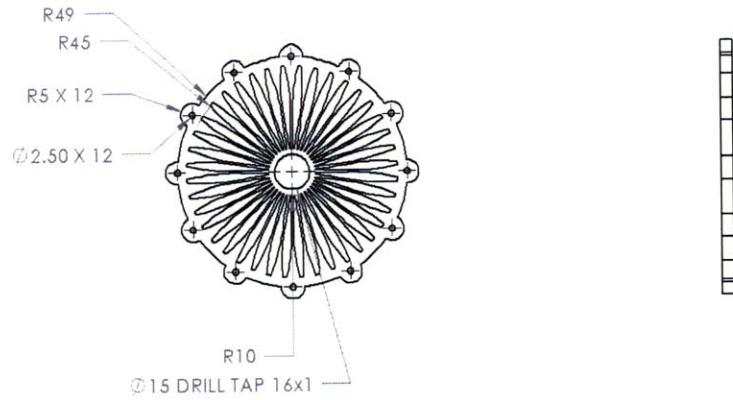


Figure 5.11: A CAD drawing of the BEAU's flexure with relevant dimensions.

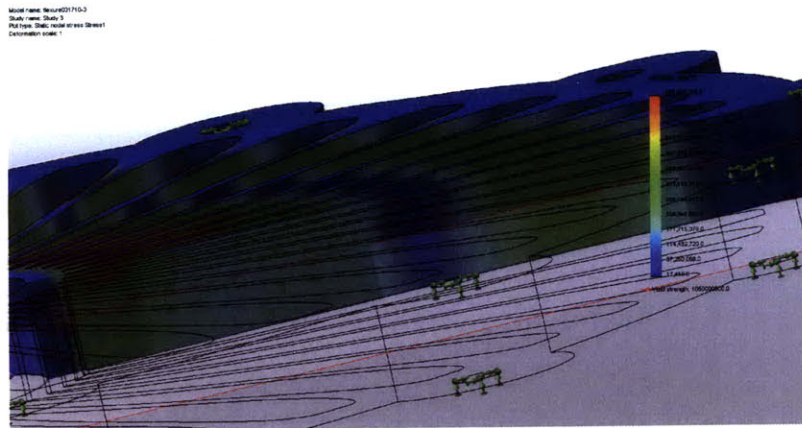


Figure 5.12: The stress plot from an FEA analysis of the radial flexure

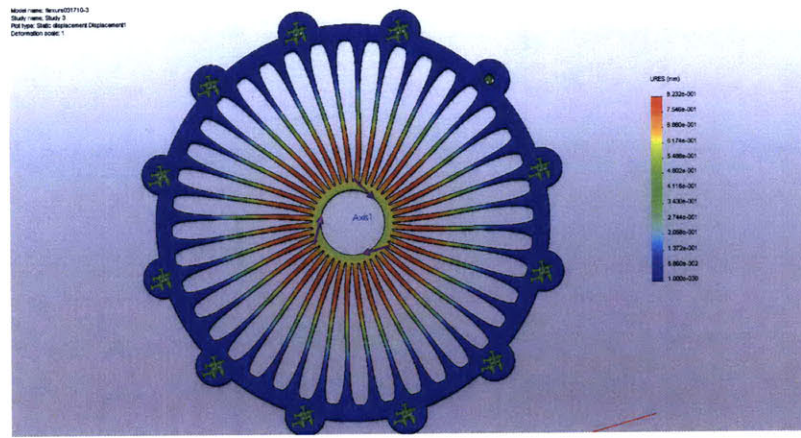


Figure 5.13: The displacement plot from an FEA analysis of the radial flexure.

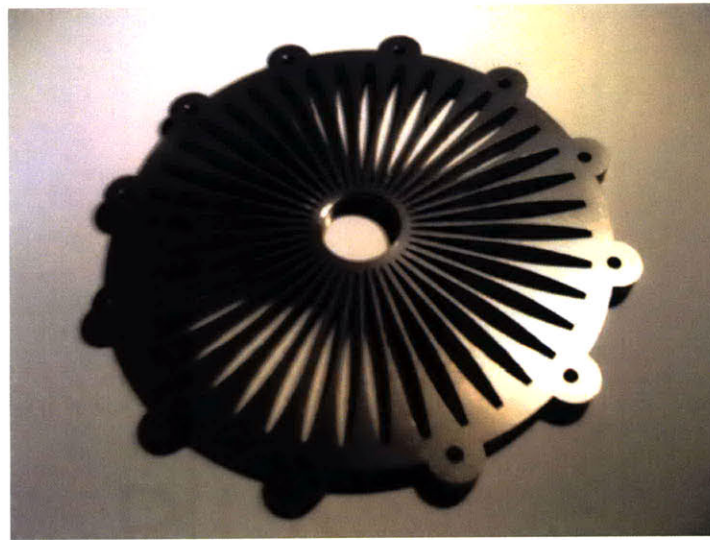


Figure 5.14: The completed radial flexure for the BEAU for use as a torque sensor.

---

## 6.0. EVALUATION OF OBJECTIVES MET THROUGH DESIGN AND ENGINEERING AND CONCLUDING REMARKS

In this thesis the author seeks to show how the BEAU's design meets the goals set forth in Section 1.3. The BEAU is shown to be designed in a way that allows it to be completely self-contained while maintaining a rich feature set equal to or surpassing the state of the art in electric bicycles. The size of the BEAU meets the standard rear fork width for all new bicycles that adhere to the rear fork standardization and any other bicycle with a rear fork that can fit a 122mm hub. Form language of the whole was kept in mind while designing the external surfaces of the BEAU. The form of the BEAU matches the general form of a bicycle. The BEAU does not require any additional knowledge to use than a normal bicycle<sup>1</sup>.

The work with the BEAU makes the following contributions:

1. Methods of custom motor design for use in academic/prototyping settings
2. Rotary flexure design guidelines and theory
3. A novel method of measuring torque through flexure deflection on rotating platforms
4. A custom motor controller useful for a variety of BLDC motor applications
5. Enhanced user experience through intelligent control systems

The custom motor design research helps to provide a fast, simple method to arrive at a reasonable estimate of motor size, number of poles and number of slots for a brushless motor stator design. After working through these steps, it is not recommended that a stator be designed and fabricated for a custom motor unless it is absolutely necessary. Generally a stator of the right size can be found and custom wound, and this will save large amounts of time in any endeavor requiring a custom motor.

The rotary flexure analysis presented in this document outlines the methods to produce many types of small angle deflection rotary flexures. This analysis can be used to quickly estimate the usually hard to determine parameters of flexure design in the closed form, and detailed analysis can be done numerically and subsequently tested using FEA software. Also, flexures requiring larger deflections can make use of the same analysis techniques, by simply ignoring the small angle approximations<sup>2</sup>.

---

<sup>1</sup>Regenerative braking requires that the user know to pedal backwards, but it is not necessary for them to use regenerative braking in order to slow down as the normal bicycle brakes are unmodified

<sup>2</sup>Be warned: larger angles of deflection do work with the small angle approximation solved out, but axial strain begins to play a non-negligible role in total stress. Axial strain cannot be solved for in the closed form, but is not difficult to calculate numerically using software such as Matlab.

While several methods exist for measuring torque – and measuring it on a rotating reference with respect to the signal processing location, the flexure based system offers several advantages that these systems do not. The flexure based torque measurement is immune to electrical noise, highly repeatable, and does not wear. Also the addition of the flexure to the drive system pathway of the BEAU added a critical spring element to the system dynamics, making it much easier and more predictable to control.

While this has only been tested with previous manifestations of the BEAU that have reached completion, the BEAU and electric bicycles like it (for example, the GreenWheel) have had very positive responses from all those who have had a chance to ride one. The ability to get on a bicycle, pedal, and have it increase the torque output is very satisfying to the user. Several demonstrations around the lab have resulted in roughly 50 test rides by visitors. Most are surprised, happy, and excited by the experience. It is easy to see why.



---

## BIBLIOGRAPHY

- [1] M. Shakeri A. Jabbari and A. Nabavi. Shape optimization of permanent magnet motors using the reduced basis technique. *World Academy of Science, Engineering and Technology*, 2009.
- [2] Atmel Corporation. *AVR444: Sensorless control of 3-phase brushless DC Motors*, 2006.
- [3] Robert John Calvet. Rotary flexure. United States Patent 6,146,044, August 1998.
- [4] Y. Dote and S. Kinoshita, editors. *Brushless Servomotors: Fundamentals and Applications*. Clarendon Press, 1990.
- [5] J. F. Gieras and M. Wing. *Permanent Magnet Motor Technology: Design and Applications*. Marcel Dekker, Inc., second edition, revised and expanded edition, 2002.
- [6] Jens Hamann Hans Grob and Georg Wiegartner. *Electrical Feed Drives in Automation: Basics, Computation, Dimensioning*. Publicis MCD Corporate Publishing, 2001.
- [7] D.C. Hanselman. *Brushless Permanent-Magnet Motor Design*. McGraw-Hill, 1994.
- [8] J.R. Hendershot. Brushless d.c. motors without permanent magnets. In *18th Annual Symposium on Increment Motion Control Systems and Devices*, 1989.
- [9] R.C. Hibbeler. *Mechanics of Materials*. Peason Prentice Hall, 6th edition edition, 2005.
- [10] Jeremy Hsu. A foldable electric bicycle for your urban commuting needs. October 2009.
- [11] Chen-Hsien Fan Jhe-Hong Wang and Chao-Chieh Lan. A two-way flexural rotation manipulator using opposing shape memory alloy wires. In *IEEE/IASME International Conference on Advanced Intelligent Mechatronics*, 2009.
- [12] M. Kihara. Introduction to electromagnet design. June 2000.
- [13] Peter Moreton. *Industrial Brushless Servomotors*. Newnes, 2000.
- [14] M.M.A. Rahman and Ken Ziba. A brushless dc motor design approach to limit magnetic saturation in generation mode. In *ASEE North Center Section Conference*. American Society for Engineering Education, 2008.
- [15] N. C. Dahl S. H. Crandall and T. J. Lardner, editors. *An Introduction to the Mechanics of Solids*. McGraw-Hill, second edition with si units edition, 1999.

- [16] Jianwen Shao. Direct back emf detection method for sensorless brushless dc (bldc) motor drives. Master's thesis, Virginia Polytechnic Institute and the State University, September 2003.
- [17] Stuart T. Smith. *Flexures: Elements of Elastic Mechanics*. Gordon and Breach Science Publishers, 2000.
- [18] Jacob Tal. *Motion Control by Microprocessors*. Galil Motion Control Inc, 1990.
- [19] Richard Valentine. *Motor Control Electronics Handbook*. McGraw-Hill, 1998.
- [20] Anish Varsani. Low cost brushless dc motor controller. University of Queensland Thesis, November 2003.
- [21] R.G. Budynas. W.C. Young. *Roark's Formulas for Stress and Strain*. McGraw-Hill, Boston, 7 edition, 2002.
- [22] Carolyn Whelan. Electric bikes are taking off. March 2007.